Transcriptome profiling of the elongating internode of cotton (Gossypium hirsutum L.) seedlings in response to mepiquat chloride

Li Wang
Henan Normal University
Ying Yin
Henan Normal University
Li-Feng Wang
Henan Normal University
Menglei Wang
Henan Normal University
Miao Zhao
Henan Normal University
Ye Tian
Henan Normal University
Yong-Fang Li (li_yongfang@hotmail.com)
Henan Normal University https://orcid.org/0000-0003-4659-8637

Research article

Keywords: Mepiquat chloride, Cotton seedlings, Internode, Phytohormone, Secondary metabolism, Transcription factors, Cell division, Cell expansion

Posted Date: August 14th, 2019

DOI: https://doi.org/10.21203/rs.2.12849/v1

Version of Record: A version of this preprint was published at Frontiers in Plant Science on January 28th, 2020. See the published version at https://doi.org/10.3389/fpls.2019.01751.

Abstract

Background The plant growth retardant mepiquat chloride (MC) has been extensively used to produce compact plant canopies and increase yield in cotton (Gossypium hirsutum L.). Previous studies mainly focused on the role of gibberellins (GA) in MC-induced growth inhibition of cotton. However, the molecular mechanism underlying MC-induced growth retardation has remained largely unknown. Results In the present study, we conducted histological, transcriptomic, and phytohormone analyses of the second elongating internodes of cotton seedlings treated with MC. Histological analysis revealed that the MC-mediated shortening of internodes was caused by the suppression of cell division and decrease in cell length; this phenotype was confirmed by transcriptome profiling. Many genes related to cell growth were significantly downregulated in MC-treated internodes, such as cell cycle, cell wall biosynthesis and modification, and transport protein aquaporins. Furthermore, the expression of genes related to secondary metabolism, especially lignin and flavonoid, was down-regulated by MC treatment. The expression of genes related to GA, auxin, brassinosteroid (BR), and ethylene metabolism and signaling was remarkably suppressed, whereas that of genes related to cytokinin (CK) and abscisic acid (ABA) metabolism was induced by MC. Consistent with RNA-Seq analysis, significant decrease in endogenous GA, auxin, and BR content, but an increase in CK content, was observed in cotton internodes after MC treatment. In addition, many transcription factors (TFs) such as bHLH, AP2-EREBP, Orphans, MYB, GRF, and TCP were differentially regulated by MC; these TFs are associated with cell division and expansion, phytohormone signaling, and circadian rhythm. Conclusions This study provides novel insights into the molecular mechanism underlying the MC-mediated inhibition of internode elongation in cotton seedlings. MC reduces internode elongation by suppressing the biosynthesis and downstream signaling cascades of GA, auxin, and BR; altering the expression of many TFs; and further reducing cell division and expansion.

Background

Cotton (*Gossypium hirsutum* L.) is an important economic crop; it is widely cultivated worldwide for its natural fiber and oilseed. As a perennial shrub, cotton plants exhibit indeterminate growth. Under favorable growing conditions, excessive vegetative growth often occurs, leading to serious production problems such as auto-shading, fruit abortion, delayed maturity, and yield reduction [1]. Plant growth retardants are commonly used to inhibit excessive vegetative growth and control plant shape.

Gibberellin (GA) is a key hormone that regulates stem and internodal elongation by affecting cell division and expansion [2]. GAs promote plant growth by stimulating the degradation of DELLA proteins—the key repressors of GA signaling—by binding to the receptor—GIBBERELLIN INSENSITIVE DWARF1 (GID1)—through the ubiquitin–proteasome pathway [3]. When the content of active GAs decreases, DELLA proteins accumulate and interact with transcription factors (TFs) to suppress the expression of their target genes and further suppress cell division or cell elongation [3, 4].

Plant growth retardants have been reported to interfere with the endogenous content of not only GAs but also other plant hormones and to inhibit flavonoid biosynthesis [5]. Recent studies have shown that plant growth retardants could affect the expression of genes related to the biosynthesis and signal transduction of hormones. Paclobutrazol (PAC), uniconazole, and prohexadione-Ca (Pro-Ca) are well-known anti-GA plant growth retardants that are widely applied in various plants. PAC could reduce GA content, but increased cytokinin (CK) and abscisic acid (ABA) content in the buds and leaves of mango [6]. Uniconazole and Pro-Ca application yielded similar results in duckweed (*Landoltia punctata*) [7] and in the shoots of wheat and oilseed rape, respectively [8]. Uniconazole has been reported to inhibit brassinosteroid (BR) biosynthesis in *Pisum sativum* [9]. PAC and uniconazole could reduce ethylene levels in soybean and wheat seedlings [10] and in pineapple [11], respectively. In *Jatropha*, PAC affected the expression of genes associated with the biosynthesis and signaling of eight kinds of phytohormones [12]. Furthermore, it could inhibit the transcription of the key genes in GA, auxin, BR, ethylene, and CK signaling pathways in *Agapanthus praecox* [13]. Similarly, uniconazole altered the expression of metabolism enzymes and regulatory proteins in the GA, CK, and ABA signaling pathways in duckweed [7]. In addition to GA, auxin and BR are the major determinants of plant height; they affect cell division and elongation [3]. Defects in either their biosynthesis or signaling pathways leads to the dwarfism phenotype [3].

Apart from plant hormones, many other factors can also affect plant architecture, such as cell wall-related genes [14, 15], genes involved in secondary metabolism [16, 17], and TFs [18, 19]. In plants, cell expansion is mainly mediated by the selective loosening of cell walls, which involves the breaking of load-bearing bonds and subsequent displacement of cell wall polymers [20]. Many cell wall-related plant mutants show abnormal growth and morphogenesis [21]. Flavonoids and lignin are important secondary metabolites during plant growth and development. Flavonoids are required for internode elongation and leaf expansion in apple [16], fiber elongation in cotton [22], and pollen tube growth and development in maize and tomato [23, 24]. Lignin is a major structural component of the secondary cell wall, providing mechanical strength and hydrophobicity to the vascular system, especially in the stem [17]. Modification of its metabolism can directly affect plant growth. Lignin modification-induced dwarfism has been reported in Arabidopsis, poplar, tobacco, and alfalfa [25-27]. TFs are important regulators of plant growth and development; they activate or inhibit the transcription of downstream genes in response to environmental stimuli. Multiple TFs have been reported to alter plant architecture by regulating cell proliferation and/or expansion. For example, the members of the TCP family are typically associated with cell proliferation and expansion [28]. Growth-regulating factors (GRFs) positively regulate leaf size and stem elongation by promoting cell proliferation or expansion [19, 29]. In addition, TFs play key roles in integrating signal transduction of different phytohormones. DELLAs, members of the GRAS family, are typical examples [30]. PREs, members of the bHLH family, have been reported to positively regulate cell elongation in response to GA, BR, and auxin signaling [31].

Mepiquat chloride (MC) is a kind of plant growth retardant [32]. Unlike other plant species such as wheat, maize, and soybean, cotton is more sensitive to MC [5]; therefore, MC is commonly used in cotton to control growth, maximize yield, and improve fiber quality by reducing leaf area and shortening internodes

[33-35]. Because of its chemical structure similarity to chlorocholine chloride, the regulatory mechanism of which has been relatively well studied in plants, MC is hypothesized to function by specifically inhibiting the activity of copalyl diphosphate synthase (CPS) in the early steps of GA biosynthesis [5, 36]. Previously, we showed that MC inhibited the expression of genes related to GA metabolism and signaling pathway and reduced GA content in cotton internodes [37]; however, the transcriptional regulatory network underlying MC-mediated growth inhibition remains largely unknown. Hence, in this study, we intended to determine the signal pathways and genes associated with the growth inhibition of MC by conducting global transcriptome profiling of the elongating internodes of cotton seedlings treated with MC. The potential target genes were identified by evaluating phenotype, histology, and phytohormone metabolite levels. A better understanding the molecular mechanism of MC action may help accelerate the molecular breeding process of cotton.

Results

MC shortened cotton seedling internodes by reducing cell division and cell elongation

First, we checked the effect of MC treatment on cotton seedling growth. Cotton seedlings at the three-leaf stage were treated with foliar spray of 80 mg/L MC. Ten days after MC treatment, plant height decreased by 40 % compared to that of control plants (Fig. 1a). The height of the first, second, third, and fourth internodes (from bottom to top of the stem) decreased by 46, 55, 52, and 83 %, respectively (Fig. 1b, c). The elongation of the second internode—the first visible and youngest sub-apical internode at the time of MC treatment—was inhibited more severely than that of the first internode by MC application; therefore, the second internode was used for further study. The length of the second internode was reduced by 10, 31, 49, 53, and 55 % at 2, 4, 6, 8, and 10 d after MC treatment, respectively (Fig. 1d). The inhibition of internode elongation by MC was time-dependent.

Internode elongation involves both cell division and cell elongation. To determine the contribution of cell division and elongation to the shortening of internodes by MC application, we evaluated cell length and number along the vertical axes of the second internode at the tenth day after MC treatment. The longitudinal cells in the cortex and pith of MC-treated internodes were significantly smaller than those of control internodes (Fig. 2a, b, c, d). The average longitudinal cell length of MC-treated internodes was 27 % smaller than that of the control internodes (Fig. 2e). The cell number along the second internode of the MC-treated plants was 21 % less than that of the control plants (Fig. 2f). Therefore, MC shortened internodes by suppressing both cell division and elongation.

Overview of the transcriptome profile of the second internode in response to MC treatment

To investigate the transcriptional regulatory mechanisms underlying the inhibition of internode elongation by MC, we analyzed the transcriptome profiles of the second internodes of cotton seedlings from the control (water, 0 h) and MC-treated plants (48, 72, and 96 h after MC treatment). In all, 12 RNA-Seq libraries were constructed and sequenced. An overview of the RNA-Seq sequencing reads derived from the 12 libraries is shown in Table 1. After adaptor sequence and low-quality reads were removed,

each library generated 64.9 to 74.6 million clean reads (Table 1). All 12 libraries had a constant GC content of approximately 43 % and high Q30 percentage of approximately 94 %. The proportion of clean reads mapped to the cotton genome ranged from 94.8 to 96.2 %, and that of the uniquely mapped reads ranged from 87.3 to 89.1%. The R^2 value between biological replicate samples was greater than 0.96, which was higher than the required R^2 of 0.92 under ideal sampling and experimental conditions (Additional file 1: Figure S1). Therefore, the libraries and sequencing quality were considered to be excellent, with good repeatability among samples.

Differentially expressed genes (DEGs) in response to MC treatment

To determine the gene expression changes in the internodes resulting from MC treatment, we normalized gene expression by using the fragments per kilobase of exon per million fragments mapped (FPKM) value. Transcripts with |log2 (fold change)|>1, false discovery rate (FDR) <0.05 and more than 1 FPKM in at least one sample of each comparison were considered as DEGs. Compared with that in the control (0 h), 1378 (645 upregulated and 733 downregulated), 2751 (1086 upregulated and 1665 downregulated), and 3459 (1479 upregulated and 1980 downregulated) DEGs were identified after MC treatment for 48, 72, and 96 h, respectively (Fig. 3a). The numbers of both up- and down-regulated DEGs increased with time. As shown in the Venn diagrams (Fig. 3b), 1058 (456 upregulated and 602 downregulated) DEGs were shared between 48 vs. 0 h and 72 vs. 0 h; 1675 (560 upregulated and 1115 downregulated) DEGs, between 72 vs. 0 h and 96 vs. 0 h; and 849 (323 upregulated and 526 downregulated) DEGs, between 96 vs. 0 h and 48 vs. 0 h. Among them, 273 and 490 genes were constantly induced or suppressed by MC treatment, respectively.

Functional analysis of the DEGs in response to MC

To better understand the potential function of DEGs responding to MC application, we conducted Gene Ontology (GO) and Kyoto Encyclopedia of Genes and Genomes (KEGG) enrichment analyses for pairwise comparisons. GO enrichment was annotated according to biological process, cellular component, and molecular function (Additional file 2: Fig. S2). In general, for the biological process and molecular function groups, enrichment patterns of DEGs were similar at 48, 72 and 96 h. In the biological process category, the most dominant terms were “single-organism process,” “response to stimulus,” and “response to abiotic stimulus.” In the molecular function category, the most highly represented GO terms were associated with “binding,” “transcription factor activity, sequence-specific DNA binding,” and “nucleic acid binding transcription factor activity.” However, in the cellular component category, the top three enriched GO terms were different among the DEGs at the three time points: “chloroplast part,” “plastid part,” and “thylakoid” were dominantly enriched at 48 h; “cell part,” “cell,” and “cell periphery” were enriched at 72 h; whereas “chromatin,” “chromosomal part,” and “chromosome” were enriched at 96 h.

For the KEGG pathway enrichment analysis, 89, 73, and 82 pathways were categorized from pairwise comparisons between 48 vs. 0 h, 72 vs. 0 h and 96 vs. 0 h, respectively (Additional file 3: Table S1). The top 20 enriched KEGG pathways of each comparison are shown in Fig. 4. The most significantly enriched

KEGG pathways in the 48 vs. 0 h DEGs was photosynthesis-antenna proteins, followed by circadian rhythm-plant, biosynthesis of secondary metabolites, metabolic pathways, and thiamine metabolism. Five KEGG pathways were identified to be significant for the DEGs from the 72 vs. 0 h as well as 96 vs. 0 h comparison, which included biosynthesis of secondary metabolites, plant hormone signal transduction, fatty acid elongation, circadian rhythm-plant, and photosynthesis-antenna proteins.

DEGs related to cell cycle and cell expansion

Based on the reduced cell number and length in MC-treated internodes, we investigated the changes in the expression of genes related to cell cycle and cell wall. In total, 57 DEGs were found to be related to cell cycle and cell division (Fig. 5a, Additional file 4: Table S2). Interestingly, most of these genes were significantly downregulated, including cyclin genes (*CYCA1;1*, *CYCA2;2*, *CYCA2;3*, *CYCA3;2*, *CYCB2;4*, *CYCD3;1*, *CYCD3;2*, *CYCD4;1*, *CYCU1;1*, *CYCU2;1*, *CYCU4-1*), cyclin-dependent kinase B1;2 (*CDKB1;2*), cyclin-dependent kinase regulatory subunit 1 (*CKS1*), E2F transcription factor-like (*E2FF*), G2/mitotic-specific cyclin-1 (*CCNB1*), peptidyl-prolyl cis–trans isomerase (*FKBP65*), cell division control proteins (*CDC2*, *CDC7*, *CDC45)*, cytochrome P450 78A (*CYP78A3*, *CYP78A5*, *CYP78A7*), syntaxin-related protein (*KNOLLE*), mitotic spindle checkpoint protein (*BUBR1*), MFP1 attachment factor 1 (*MAF1*), and meiotic nuclear division protein 1 (*MND1*). However, nine cell cycle-related genes were upregulated, such as cyclin-dependent kinase inhibitor (*KRP6* and *KRP7*) and cell number regulator 1 (*CNR1*; Additional file 4: Table S2).

Cell wall architecture is a key determinant of plant growth. We identified 75 DEGs involved in the biosynthesis and modification of cell wall (Fig. 5b, Additional file 5: Table S3). Most of these genes were highly expressed in the control internodes, such as cell wall proteins [arabinogalactan peptides (*AGPs*) and fasciclin-like arabinogalactan proteins (*FLAs*)], α-expansins (*EXPAs*), and xyloglucan endotransglycolase/hydrolases (*XTHs*). Among these DEGs, 45 genes were significantly downregulated by MC, including three cellulose synthase-like protein G3 (*CSLG3*), one glucuronoxylan glucuronosyltransferase 7 (*IRX7*), two pectinesterase (*PME68*), five pectinesterase/pectinesterase inhibitor (*PMEI*), three galacturonosyltransferase-like (*GATL1*, *GATL7*, *GATL9*), four AGPs (*AGP20*, *AGP30*), four FLAs (*FLA2*, *FLA8*), three leucine-rich repeat extensin-like protein (*LRX2*, *LRX4*), one BURP domain-containing protein 17 (*BURP17*), one putative cell wall protein, six *EXPAs* (*EXPA4*, *EXPA8*, *EXPA15*), and twelve *XTHs* (*XTH2*, *XTH8*, *XTH9* and *XTH32*). Notably, the expression of cell wall protein-encoding genes, *BURP17*, *LRX4*, *EXPAs* (*Gh_D10G1145*, *Gh_A10G2323* and *Gh_D05G2934*), and *XTHs* (*Gh_D02G0220*, *Gh_A10G0146*, *Gh_A11G2885*, and *Gh_D11G3271*) showed more than 2-fold down-regulation at 96 h after MC treatment.

Cell division and expansion require the continuous uptake of water to maintain turgor pressure. Aquaporins (AQPs) play crucial roles in the transport of water and other small molecules across membranes in plants [38]. According to sequence similarity and sub-cellular localization, AQPs are divided into five subgroups: plasma membrane intrinsic proteins (PIPs), tonoplast intrinsic proteins (TIPs), nodulin26-like intrinsic proteins (NIPs), small basic intrinsic proteins (SIPs), and X intrinsic

proteins (XIP) [39]. PIPs can be further divided into PIP1 and PIP2, on the basis of sequence similarity. To assess whether and which subfamily members of AQPs are affected by MC treatment, we analyzed the differentially expressed AQPs. Our RNA-Seq data showed that some members of *PIPs* and *TIPs* were highly expressed in the internodes of control plants (Fig. 5c, Additional file 6: Table S4). In contrast, 19 *PIPs* and 7 *TIPs* were consistently suppressed after MC treatment, and only three *PIPs* were induced by MC (Fig. 5c). The expression level of three *PIPs* (*Gh_A01G1843*, *Gh_D09G1409*, and *Gh_D01G2086*) and three *TIPs* (*Gh_D03G1253*, *Gh_D10G2205*, and *Gh_A10G1912*) was decreased by more than 2-fold. The decreased expression of *PIPs* and *TIPs* may have contributed to the inhibition of internode elongation by MC.

DEGs related to hormone metabolism and signal transduction

To investigate the roles of hormones in the inhibition of internode elongation by MC, we identified DEGs involved in the phytohormone metabolism, transport, and signal transduction pathways by comparing the profiles after and before MC treatment. About 155 hormone-related DEGs were detected after treatment with MC (Fig. 6, Additional file 7: Table S5). Most of these genes belonged to auxin metabolism and response pathways, followed by GA, ethylene, CK, and ABA; relatively fewer DEGs were related to salicylic acid (SA) and jasmonic acid (JA; Fig. 6). Most of the DEGs showed decreased expression except for the CK pathway-associated DEGs, which were generally induced by MC treatment (Fig. 6).

Thirty-two DEGs related to GA were found to be responsive to MC application (Fig. 6a). In the GA metabolism pathway, seven DEGs were found to be downregulated after MC treatment, including one biosynthetic gene (*KAO*, *Gh_Sca030829G01*) and six catabolic genes (five *GA2ox1* and one *CYP714A1*), whereas genes encoding another KAO (*Gh_A06G1386*), two ent-copalyl diphosphate synthase (*KS*), one GA 20 oxidase 2 (*GA20ox2*), and one GA 2 oxidase2 (*GA2ox2*) were upregulated by MC. In the GA signal transduction pathway, 14 genes encoding GRAS family regulatory proteins, including DELLA (*GAI*, *RGA2*, *SCR*, *SHR*, and *PAT1*), and genes encoding GID1 were downregulated at different time points (Additional file 7: Table S5).

Of the 39 DEGs related to auxin pathway, the genes related to auxin biosynthesis (*TAR2*), catabolism (*GH3*), signaling (*TIR1*, *ARF9*, *AUX22*, *AUX6B*, *AUX15A*, *AUX10A*, *IAA4*, *IAA14*, *IAA29*, and *IAA26*), and transport (*PIN1*, *PIN5* and *PIN6*) were downregulated at different time points (Fig. 6b). Eight genes encoding auxin-responsive proteins, including *SAUR66*, *SAUR20*, and *SAUR71*, were also significantly downregulated (Additional file 7: Table S5).

Expression of 23 DEGs involved in CK biosynthesis, modification, transport, and signaling was altered in response to MC (Fig. 6c). *IPT3* (*Gh_A11G3078*), encoding a rate-limiting enzyme in CK biosynthesis, was upregulated by 2.9-, 3.2-, and 3.6-fold at 48, 72, and 96 h after MC treatment, respectively, whereas another *IPT3 (Gh_D11G3514)* was downregulated only at 48 h after treatment. *Gh_D11G1669*, a cytokinin hydroxylase (*CYP735A1*), was significantly induced by MC treatment. The expression of four orthologs of CYTOKININ OXIDASES/DEHYDRO-GENASES (*CKX6* and *7*) involved in the irreversible degradation of CKs was significantly upregulated at different time points, and only *CKX1* was downregulated. The gene

encoding CK transporter purine permease 11 (*PUP11*) was also upregulated. The expression of *UGT76C2*, which encodes a glycosyltransferase that catalyzes the *N*-glycosylation of CK, was downregulated. The expression of three genes (*LOG3* and *LOG5*) encoding CK-activating enzymes was significantly decreased, especially at 96 h after MC treatment. ARRs are associated with CK signal transduction pathway; nine induced ARR genes (two B-type *ARRs*, five A-type *ARRs*, and two *B-ARR-like* genes) and four suppressed *ARR-like* genes were identified after MC treatment (Additional file 7: Table S5).

Six DEGs were found to be related to ethylene biosynthesis (Fig. 6d). Among them, a gene encoding one *S*-adenosyl methionine (SAM) synthase, one 1-aminocyclopropane-1-carboxylate (ACC) synthase (*ACS*), and one homolog of ACC oxidase (*ACO*) were significantly downregulated in response to MC; interestingly, the *ACO* homolog was downregulated by 2.0- and 5.2-fold at 72 and 96 h, respectively. However, three ACO genes were upregulated, especially at 48 h after MC treatment. In the ethylene-response pathway, eighteen DEGs were found to be downregulated by MC, including one *ETR2*, one *EBF1*, fourteen ethylene-responsive TFs (*ERF*, *WRI1*, *TINY*, *AIL6*, *ANT*, *RAP23*, and *CRF5*), and two REVERSION-TO-ETHYLENE SENSITIVITY1 (*RTE1*) genes (Additional file 7: Table S5).

In the ABA biosynthesis pathway, one gene encoding 9-cis epoxy carotenoid dioxygenase3 (NCED3) and one ABA 8′-hydroxylase (ABAH) encoding gene were upregulated by MC, whereas one zeaxanthin epoxidase (*ZEP*) gene and two *ABAHs* were consistently suppressed (Fig. 6e). Fifteen ABA signaling-related genes were identified as DEGs, with eight downregulated genes (*PYL4*, *PYL6*, *PP2C27*, *PP2C34*, and *PP2C38*) and five upregulated ones (*ABI*5, *PP2C35*, and *PP2C59*; Additional file 7: Table S5).

Two *CYP90A1*/*CPD* (constitutive photomorphogenesis and dwarfism) genes involved in BR biosynthesis were significantly downregulated by MC treatment (Fig. 6f). However, *Gh_A04G0959* (*BAK1*), encoding a receptor kinase mediating BR signaling, was upregulated 96 h after MC treatment. Five BR signaling components BR-ENHANCED EXPRESSION (*BEE*) were significantly downregulated by MC treatment, including one *BEE1*, two *BEE2*, and two *BEE3* (Additional file 7: Table S5).

The expression of *Gh_A12G2643*, isochorismate synthase 1 (ICS1) involved in SA biosynthesis; *Gh_D12G0595* and *Gh_A12G0584*, salicylate carboxymethyltransferase (SAMT) related to the conversion of SA to SA methyl ester; and *Gh_D11G1910*, salicylic acid-binding protein 2 (SABP2) converting MeSA to SA, was suppressed by MC (Fig. 6g). In the SA response pathway, one *NPR3*, an SA receptor, was significantly upregulated. In the JA biosynthesis and signaling pathway, only two allene oxide synthase *AOS*/*CYP74A* genes were downregulated by MC treatment (Fig. 6h).

DEGs related to lignin and flavonoid metabolism

KEGG enrichment showed that DEGs involved in secondary metabolism were overrepresented in response to MC treatment. In this study, we mainly focused on the DEGs related to lignin and flavonoid metabolism, which are associated with plant growth [16, 17]. The biosynthetic pathways leading to lignin and flavonoid diverge at the common intermediate *p*-coumaroyl CoA. A total of 37 genes involved in lignin biosynthesis were differentially expressed in the internodes between MC-treated and control plants

(Fig. 7a, Additional file 8: Table S6). Among these genes, 22 DEGs were downregulated by MC, including two 4-coumarate-CoA ligase (*4CL*), one 4-coumarate-CoA ligase-like (*4CLL*), two caffeoylshikimate esterase (*CSE*), four shikimate *O*-hydroxycinnamoyltransferase (*HCT*), one caffeic acid 3-*O*-methyltransferase (*COMT*), one cinnamyl alcohol dehydrogenase (*CAD*), one cinnamoyl-CoA reductase (*CCR*), four laccase (*LAC*), and six peroxidase (*PRX*). Notably, one *HCT* showed more than 2.5-fold down-regulation after MC treatment. Fifteen DEGs were upregulated, including one *4CL*, two *CSE*, two *COMT*, one *CAD*, one *LAC*, and eight *PRX*.

In total, 14 DEGs involved in flavonoid biosynthesis were identified (Fig. 7b, Additional file 8: Table S6). Among these DEGs, 10 were downregulated by MC, including two *CHS*, one leucoanthocyanidin dioxygenase (*LDOX*), two flavonol synthase (*FLS*), one flavanone 3-dioxygenase, one flavonoid 3-*O*-glucosyltransferase, two anthocyanin 5-aromatic acyltransferase, and one flavonol sulfotransferase-like. The catalysis of CHS is the initial step of the flavonoid biosynthesis pathway. Interestingly, two *CHS* genes showed significant down-regulation at different time points after MC treatment, with more than 3-fold down-regulation both at 72 and 96 h.

Differentially expressed TFs

The changes in gene expression level are known to be closely related to the alterations of TFs. We identified 497 differentially expressed TFs that belong to 46 different families, including MYB, Orphans, bHLH, AP2-EREBP, HB, WRKY, NAC, bZIP, GRAS, AUX/IAA, GRF, and TCP, in response to MC treatment (Additional file 9: Table S7). Some important TFs are shown in Fig. 8. Most of the MYBs were downregulated (Additional file 9: Table S7), including genes functioning in plant circadian clock and ABA accumulation [40] and those associated with the ABA signal pathway [41]. The bHLH TFs play important roles in the control of cell elongation. Five *BEEs* (*BEE1*, *BEE2*, and *BEE3*), BR early-response genes and associated with BR-regulated cell elongation [42], and four *PREs* (*PRE5*, *PRE6*) were significantly downregulated. In addition, four bHLH36 showed more than 3.2-fold up-regulation at different time points after MC treatment. The expression of AP2/EREBP family TFs was altered in MC-treated internodes. Twelve ERF genes involved in ethylene signaling and response pathway were also downregulated in response to MC. Two *ANT* and *CRF5* genes each were downregulated. Among Orphans family TFs, fourteen *BBX* (*BBX19*, *BBX24*, *BBX32*) TFs were significantly downregulated by MC. One *ETR2*, an ethylene receptor, was significantly downregulated. In contrast, ten *CONSTANS*, positive regulators of photoperiodic flowering, and seven *ARR* (*ARR2*, *ARR8*, *ARR9* and *ARR14*) genes were significantly upregulated. Moreover, 14 NAC TFs were upregulated in response to MC (Additional file 9: Table S7). The HB family TFs such as *ATHB*, *KNAT6*, and *HAT* were significantly downregulated, except for *HAT22*, which was upregulated. The majority of WRKY family TFs was upregulated, such as *WRKY18, WRKY21*, *WRKY23*, *WRKY4*0, *WRKY51*, *WRKY57*, and *WRKY70* (Additional file 9: Table S7). Nine bZIP members, including *ABI5*, *bZIP34*, *bZIP61*, Ocs element-binding factor 1(*OCS1*), and *HY5*, were significantly downregulated (Additional file 9: Table S7). The transcription level of all GRF family TFs decreased gradually after MC treatment. Remarkably, most of *GRF* genes showed more than 2-fold down-regulation 96 h after MC treatment compared with that in the control. Six TCP TFs were downregulated.

Validation of RNA-Seq data by using qRT-PCR

To validate the reliability of RNA-Seq data, we randomly selected 20 DEGs related to phytohormone biosynthesis and signal transduction pathways and cell cycle-related genes and TFs for qRT-PCR analysis (Fig. 9). The expression profiles of these genes from both qRT-PCR and RNA-Seq analysis were highly consistent, indicating the reliability of the RNA-Seq data.

Changes in endogenous hormone content in the second internode after MC treatment

Numerous DEGs associated with hormone biosynthesis and signal transduction pathway were enriched. To investigate whether MC affects endogenous hormone content, we quantified GA, IAA, BR, and CK (*trans*-zeatin) levels in the second internode of control and MC-treated plants. The levels of GA1, GA3, and GA4 were reduced by 78, 57, and 29 % in MC-treated plants 6 days after treatment, respectively (Fig. 10a). Similarly, endogenous IAA and BL, the most biologically active BRs, were reduced by 46 and 36 %, respectively (Fig. 10b, c). In contrast, endogenous CK level was increased by 95 % in MC-treated plants (Fig. 10d). These data indicate that the dwarfism caused by MC is closely related to the reduction of endogenous GA, IAA, and BR content.

Discussion

MC has been the most successful and widely used plant growth regulator in cotton; it allows to compact plants by reducing internode length and leaf size [33-35]. Previously, we showed that MC reduced the synthesis of GA, resulting in the suppression of cell elongation in the internodes of cotton seedlings [37]. In this study, we analyzed the global transcriptional changes in the second elongating internodes of cotton seedlings in response to MC to elucidate the other potential mechanisms underlying MC-induced internode elongation.

MC reduced internode elongation by inhibiting cell division and expansion

As previously reported [33-35], MC significantly reduced plant height by shortening internode length (Fig. 1). MC has been shown to limit internode elongation mainly by obstructing cell elongation [37, 43]. Our histological observation indicated that cell number and length of internodes, which are related to cell division and cell expansion, respectively, were both significantly reduced by MC (Fig. 2). Consistent with the results of microscopic analysis, transcriptome data showed that numerous genes related to cell cycle and cell wall were altered by MC treatment. In plants, the cell cycle is mainly regulated by CDKs and cyclins [44]. A-, B- and D-type cyclins mainly regulate the S and G2/M phases, and B-type CDKs are specifically expressed in G2 and M phase [44]. Our study showed that B-type CDKs; CKS1; A-, B-, D-, and U-cyclins; and G2/mitotic-specific cyclins were downregulated by MC (Fig. 5a). Moreover, five genes encoding cell division control proteins, which primarily target cell cycle regulators for proteolysis, were downregulated [45]. Cell cycle inhibitor genes (*KRP6* and *KRP7*) were upregulated by MC (Fig. 5a); this could also contribute to the reduced cell division, as cell cycle inhibitors can inactivate CDKs and function as inhibitors of cell proliferation [44]. The *CYP78A* family members, including *CYP78A5*, *CYP78A6*, and

CYP78A7 in Arabidopsis [46, 47] and *TaCYP78A3* [48] and *TaCYP78A5* [49] in wheat, have been shown to control reproductive organ growth and seed development by promoting cell proliferation. Silencing of *TaCYP78A3* or *TaCYP78A5* caused a reduction in seed size owing to the reduced cell numbers in the seed coat of wheat [48, 49]. In this study, six *CYP78A* family members showed more than 2-fold down-regulation 96 h after MC treatment, suggesting that they might control internode elongation by regulating cell proliferation in cotton. CNR1 has been shown to be a negative regulator of cell number, which is expressed mainly in the vegetative tissues of maize [50]. The overexpression of *CNR1* reduced the internode length and leaf size of maize owing to the reduced cell number [50]. A cotton *CNR1* was significantly upregulated by MC (Fig. 5a), suggesting that *CNR1* is also related to internode elongation in cotton.

Cell elongation requires the selective loosening of cell walls, which are composed of cellulose, hemicellulose, and pectin, as well as proteins [20]. EXPAs and XTHs are two types of important cell wall proteins that are involved in cell elongation. EXPAs can break the hydrogen bonds linking cellulose and hemicellulose, especially xyloglucan, thereby loosening the cell wall [14]. XTHs can cleave and reattach xyloglucan polymers [51]. In our previous study, we showed that MC suppressed the expression levels of *GhEXP* and *GhXTH2* in cotton internodes within 2–10 d after treatment [37]. In this study, six *EXPs* and twelve *XTHs* were found to be significantly downregulated by MC (Fig. 5b). In addition, other cell wall-related genes such as *PME*s, *FLA*s, and *AGP*s were also downregulated by MC treatment (Fig. 5b). PMEs catalyze the demethyl esterification of pectin and regulate pectin reconstruction, thereby increasing the extension of cells [20]. High PME activity was required for cell elongation in germinating shoots [52]. AGPs have been reported to be involved in cell elongation and can be induced by BR [53, 54]. FLAs, cell surface glycoproteins, belonging to AGPs, are important for normal cell expansion [55]. In cotton, the overexpression of *GhFLA1* increases fiber length, whereas its silencing results in shorter fibers [56].

Cell growth is tightly related to the regulation of hydraulic and turgor pressure, which is associated with AQPs [38]. The significance of PIPs and TIPs in tissue elongation has been shown by a positive correlation between gene expression and cell expansion in leaves, hypocotyls, roots, reproductive organs, and fruits [57]. The expression of *AQP* genes is regulated by phytohormones such as GA and ethylene [58, 59]. The expression of *AtTIP1;1* in Arabidopsis can be induced by exogenous GA_3 [58]. Ethylene can inhibit cell expansion of rose petals, at least partially, by suppressing the expression of *RhPIP2;1* [60]. In this study, most *PIPs* and *TIPs* exhibited reduced expression in the internodes shortened by MC treatment (Fig. 5c), accompanied with the decreased content of GAs (Fig. 10a), indicating that MC-induced alteration of GAs may affect the expression of *PIPs* and *TIPs*, which further affected internode elongation.

The biosynthesis and signaling transduction of multiple hormones were remarkably altered by MC treatment

Previously, we showed that MC suppressed the expression of GA biosynthesis genes (*GhCPS*, *GhKS*, *GhGA20ox*, and *GhGA3ox*), GA catabolism genes (*GhGA2ox*), and signal transduction genes (*GAI*) [37]. In

this study, RNA-Seq profiles showed similar expression changes in GA metabolism and signaling genes. The majority GA metabolism- and signal transduction-associated DEGs were downregulated by MC, including the GA biosynthesis gene (*KAO1*), GA catabolism genes (*GA2ox1*, *CYP714A1*), and GA signal transduction genes (*RGA2*, *GAI*, *GID1*; Fig. 6a). Endogenous GA_1, GA_3, and GA_4 contents were remarkably reduced by MC 6 d after treatment (Fig. 10a), consistent with the findings of our previous study showing that endogenous GA_3 and GA_4 levels were decreased in cotton internodes within 2–10 d after MC treatment [37]. Many studies have shown that the decreased GA levels can promote the accumulation of DELLA proteins, which can in turn repress the expression of *DELLAs* [3, 4]. In *Arabidopsis*, RGA and GAI are the major DELLA proteins repressing GA-regulated stem elongation [61]. In addition, most crosstalk between GA and other phytohormones is mediated by DELLAs via direct protein–protein interaction [3, 4] .

Auxin also plays important roles in the determination of plant height by regulating cell expansion and cell division. The levels of free active auxin are determined by biosynthesis, conjunction, and polar transport in plant organs. Our RNA-Seq data showed that the expression of genes related to auxin biosynthesis (*TAR2*) and conjunction (*GH3*) were remarkably decreased by MC (Fig. 6b). The conversion of Trp to indole-3-pyruvate by TAR2 is the main route of Trp-dependent auxin biosynthesis [62]. The GH3 enzymes conjugate free IAA with amino acids and prevent excess auxin accumulation [63]. The expression of *GH3* is feedback regulated by free auxin levels [63]. Polarized auxin transport by PIN efflux carriers is essential for creating auxin gradients and for auxin homeostasis. In this study, the decreased expression of *PIN* family genes (*PIN1*, *PIN5*, and *PIN6*) suggested that auxin transport and homeostasis were disrupted in cotton internodes by MC treatment (Fig. 6b). Similar down-regulation of *PIN* genes was observed in *Jatropha curcas* L. flower buds after PAC treatment [12]. GA has been reported to induce the expression of *PIN* [64], whereas DELLA negatively regulates polar auxin transport by inhibiting the transcription of *PIN* [65]. Therefore, inhibited auxin transport in MC-treated internodes may be related to the reduced GA levels. Consistent with the decreased biosynthesis and transport of auxin, reduced IAA levels were observed in MC-treated internodes 6 d after treatment (Fig. 6b and Fig. 10b). Furthermore, the down-regulation of auxin signaling genes such as auxin receptor *TIR1*, auxin response factor *ARF*, and *AUX/IAA* transcriptional repressors indicated that auxin signal transduction was somehow blocked in cotton internodes by MC. Similarly, in *Agapanthus praecox*, free IAA content and auxin-regulated transcription process were remarkably decreased in the dwarfing scape after PAC treatment [13]. In litchi, auxin response genes such as *AUX/IAA*, *GH3*, and *SAUR* were suppressed at the flowering stage after uniconazole treatment [66].

BRs are essential for stem elongation, and BR-deficient mutants exhibit characteristic dwarfism and compact stature [3]. CPD is crucial for BR biosynthesis [66]. In Arabidopsis, the *cpd* mutant showed reduced bioactive castasterone and brassinolide (BL) and exhibited severe dwarf phenotypes [66]. In this study, MC significantly inhibited the expression of two *CPDs*, as well as caused a remarkable reduction in BL content in MC-treated internodes (Fig. 6f and Fig. 10c). MC significantly downregulated *BEE1*, *BEE2*, and *BEE3*, whereas upregulated *BAK1*. This suggests that BAK1 is shared with other signaling pathways such as plant immunity [67]. In Arabidopsis, the *bee1 bee2 bee3* triple mutant showed similar phenotype

to that of known BR mutants [42]. In poplar, the overexpression of *BEE3-like* gene increased plant height and internode length [68].

GAs and CKs are known to antagonistically regulate multiple developmental processes such as hypocotyl and internode elongation [69]. Unlike GA, auxin, and BR, most CK-related DEGs were upregulated by MC (Fig. 6c). In this study, MC-induced increase of CTK content was consistent with the up-regulation of CK biosynthesis (*IPT3* and *CYP735A1*) and transport genes (*PUP11*) in cotton internodes (Fig. 6c and Fig. 10d). Active CKs are degraded mainly by CKX, which can be induced by exogenous CTK owing to feedback mechanisms [70]. Therefore, the MC mediated upregulation of *CKX1*, *CKX6*, and *CKX7* might be attributed to the increased CK levels in cotton internodes. A-type ARR genes are the primary responsive genes in CK signaling pathway and can be transcriptionally induced in response to cytokinin [70]. Nine of thirteen *ARR* genes were upregulated by MC in cotton seedlings, suggesting that MC affects not only CK levels but also its signaling in cotton internodes. Other plant growth retardants such as PAC, uniconazole, and Pro-Ca have been reported to increase CK levels in different plant tissues [6-8]. Increased accumulation of CK in plants could reduce stem elongation, decrease leaf area, increase chlorophyll contents, and delay leaf senescence [71].

Ethylene is known to promote internode elongation in deep-water rice plants. In cotton, ethylene is the major phytohormone that stimulates fiber cell elongation [72]. The role of ethylene in the vegetative phase internode development is not yet completely understood. During ethylene biosynthesis, SAM synthase first converts methionine to SAM [73], which is then catalyzed to ACC by ACS [73]. Finally, ACC is oxidized to ethylene by ACO [73]. Previous studies showed that anti-GA growth retardants such as PAC and uniconazole suppress ethylene synthesis by blocking ACO [10, 11]. In this study, the suppressed expression of SAM synthase, ACS, and ACO imply that MC-treated internodes have reduced ethylene levels (Fig. 6d). The expression of eighteen DEGs related to ethylene signaling, including ethylene receptor (*ETR2*) and *EBF1*, both of which can be transcriptionally induced by ethylene owing to their negative regulators in ethylene signaling, was inhibited by MC [73]. Similarly, in the PAC-treated dwarfing scape of *Agapanthus praecox*, the expression levels of ethylene signal transduction genes were markedly decreased [13]. Therefore, suppressed ethylene biosynthesis may contribute to the MC-induced internode elongation inhibition.

ABA is a negative regulator of stem elongation and the initiation and elongation of cotton fiber [74, 75]. Submergence reduced the ABA content of the elongating internodes of rice [15]. In our study, MC treatment increased the expression level of *NCED3,* which encodes a rate-limiting enzyme in ABA biosynthesis, and suppressed the expression of two *ABAH4/CYP707A4,* which encode ABA inactivation enzymes (Fig. 6e). These results implied that ABA might be accumulated in the MC-induced shortened internodes. In addition, *ABI5*, an important positive regulator of ABA signaling, was activated, and genes encoding PP2Cs and RAV1, negative regulators of ABA signaling, were suppressed, indicating an enhancement of ABA signal transduction by MC application. Lim et al. [76] reported that DELLA proteins could activate ABI5 in imbibed seeds of Arabidopsis; the induction of *ABI5* in cotton internodes by MC treatment might be attributed to the accumulation of DELLAs.

The inhibition of internode elongation by MC requires many TFs

Several TF families, including bHLH, AP2-EREBP, Orphans, MYB, GRF, and TCP, have been characterized for their regulatory roles in plant growth; they are mainly related to the triggering of downstream signaling cascades of hormones and metabolites. *BEEs* or *PREs* are involved in phytochrome signal transduction. In Arabidopsis, the overexpression of *PRE1*, *PRE5*, or *PRE6* resulted in elongated hypocotyl compared with that in the wild-type seedlings [77]. In this study, the reduced expression of five *BEEs* and six *PREs* by MC might have limited cell elongation of cotton internodes, which could be attributed to the reduced GA, BR, and auxin levels (Fig. 8).

ANT and AIL, AP2-type TFs, are positive regulators of cell proliferation and organ growth in plants. In Arabidopsis, the overexpression of *ANT* enhances organ size in leaves, floral organs, and siliques, whereas *ant* mutants show reduced size of floral organs and leaves [78]. *ANT* has been assumed to promote leaf growth by activating the expression of *CYCD3* [78]. AIL and ANT have been reported to play partially overlapping roles in several aspects of plant development [79]. Arabidopsis *ant ail6* double mutants exhibited reduced stature and smaller rosette leaves and sepals because of the reduced cell expansion or cell number [79]. In this study, MC-induced suppression of two *ANTs* and one *AIL6* may have contributed to the inhibition of cell division and cell expansion in cotton internodes (Fig. 8).

BBX proteins are the key regulators to control growth and developmental processes such as seedling photomorphogenesis and shade avoidance [80-83]. In Arabidopsis, BBX19 positively regulates growth; inhibition of its expression by using RNA interference results in reduced hypocotyl length [80]. BBX24 mediates cell elongation under shade by impairing DELLA activity, and the defective hypocotyl elongation phenotype of *bbx24-1* and *bbx24-2* mutants under shade can be completely rescued by exogenous GA_3 [81]. The overexpression of *BBX32* promoted hypocotyl growth by extending the hypocotyl elongation phase to the dark period [82]. The overexpression of *AtBBX32* in soybean altered the expression levels of soybean clock genes *GmTOC1* and LHY-CCA1-like2 (*GmLCL2*), which resulted in the increased reproductive development period and enhanced grain yield [83]. Edwards et al. [84] reported that the down-regulation of the circadian clock genes *LHY1* and *LHY2*—MYB TFs—shortened the circadian clock period, caused the misaligned expression of *CYCD3*, and resulted in the misregulation of cell division, thereby reducing the growth rate of *Populus*. In our study, the reduced expression of six *BBX19*, two *BBX24*, six *BBX32*, and six *LHY* suggested that MC might inhibit internode elongation partly by disrupting the circadian clock (Fig. 8).

GRFs, plant-specific TFs, are involved in the regulation of leaf development, stem elongation, root growth, flower development, fruit enlargement, and seed formation [85, 86]. In Arabidopsis, loss-of-function and overexpression mutants of *AtGRFs* exhibited small and large leaves, respectively [87]. In maize, the overexpression of *ZmGRF1* resulted in enhanced leaf size and increased cell number [88]. In *Populus*, leaf size and palisade cell size were remarkably increased and decreased in *GRF15*-overexpressing and dominant repression lines, respectively [29]. The roles of GRFs in the regulation of stem elongation were reported mainly in monocot plants. The repression of *OsGRFs* resulted in dwarf rice plants with short

internodes [19]. Some studies have shown that the expression of *GRFs* can be induced by GA and reduced by PAC [19, 89]. In this study, the repressed expression of twelve *GRFs* in the shortened internodes by MC treatment suggested that these GRFs might positively regulate internode elongation, which may be related to the reduced GA levels (Fig. 8).

The TCP family has been subdivided into classes I and II in Arabidopsis. Class I TCPs are thought to promote growth, whereas class II genes inhibit growth [90]. However, this classification is not always clear. In Arabidopsis, cell proliferation is promoted in young internodes, but inhibited in leaves, by AtTCP14—a member of class I TCPs [91]. In contrast, gain-of-function and loss-of-function mutants of class II TCP lead to increased and decreased hypocotyl cell length, respectively [92]. In the present study, the reduced expression of *TCP14*, *TCP7* (class I TCP) and *TCP4*, *TCP5* (class II TCP) in MC-treated internodes might have contributed to the inhibition of internode elongation. Davière et al. [18] showed a positive function of class I TCP factors in GA-mediated control of plant height. DELLAs can directly suppress the transcriptional activity of class I TCP proteins, which can bind directly to core cell cycle genes [18]. Therefore, the suppression of *TCP14* and *TCP7* by MC may be related to the reduced GA and accumulated DELLA (Fig. 8).

Lignin and flavonoid biosynthesis was inhibited by MC treatment

Lignin, a major structural component of the secondary cell wall; plants defective in lignin biosynthesis usually show severe growth retardation. The loss of function of CSE—catalyzing caffeoyl shikimate to caffeic acid—in *Arabidopsis* and *Medicago truncatula* results in reduced lignin levels and severe dwarfing [93, 94]. The transgenics of *alfalfa* and *Arabidopsis* with downregulated *HCT*, which catalyzes the conversion of *p*-coumaroyl-CoA to *p*-coumaroyl shikimate, are severely dwarf [27, 95]. LAC and PRX are oxidative enzymes that activate the monomers for combinatorial coupling into lignin in the cell wall [96]. Triple *lac4*/ *lac17*/ *lac11* mutants cause dwarf Arabidopsis plants with little lignin [97]. In our study, the shortened internodes caused by MC showed significantly reduced expression of most of the lignin biosynthetic genes, including *CSE*, *4CL*, *HCT*, *CCR2*, *CAD*, *LAC*, and *PRX* (Fig. 7a), suggesting that lignin biosynthesis was inhibited by MC. The GA content was found to be positively correlated with lignin formation in plants. GA treatment can directly stimulate lignin accumulation in tobacco petioles [98]. The reduction of GA content by the overexpression of *AtGA2ox1* in tobacco [98] and *AtGA2ox8* in canola [99] was accompanied by the reduced expression of lignin biosynthesis genes and reduced lignification. Björklund et al. [64] reported that lignin biosynthesis genes induced by GA were also strongly induced by IAA in *Populus*, and lignification of fibers occurs late during xylem development when both IAA and GA concentrations are low. The decreased GA and auxin contents in MC-treated internodes may inhibit lignin biosynthesis, thereby causing the dwarf phenotype of cotton seedlings.

Flavonoids have been documented to affect plant growth and development mainly by negatively regulating auxin transport [16, 100]. The important roles of flavonoid in this process were mainly discovered in plants with the reduced expression of *CHS* [16, 100]. Arabidopsis *CHS* mutants (*tt4*) showed higher shoot-to-root auxin transport and exhibited reduced plant height and stem diameter [100]. Dare et

al. [16] reported that *CHS*-silenced apple lines with shortened internode lengths, smaller leaves, and remarkably reduced growth rate also showed increased rates of auxin transport. Flavonoid metabolism has been reported to remain active in the early fiber cell elongation stage of cotton [22]. Our RNA-Seq data showed that the expression of two *CHSs* was significantly reduced (even by more than 2-fold) 48 and 72 h after MC treatment (Fig. 7b). In addition, other flavonoid genes such as *LDOX*, *FLS*, and *F3H* were significantly downregulated in response to MC. Therefore, flavonoid metabolism may be involved in the internode elongation of cotton and can be inhibited by MC treatment.

Conclusions

In the present study, histological, transcriptomic, and phytohormone analyses were conducted to better understand the mechanisms by which MC inhibits cotton internode elongation. Histological analysis showed that MC reduced internode length by inhibiting cell division and cell expansion. The dynamic transcriptome of the elongating internodes revealed 1378, 2751, and 3459 DEGs at 48, 72, and 96 h after MC treatment, respectively. DEG and phytohormone analyses suggested that MC suppressed the biosynthesis and signaling transduction of several important growth hormones, including GA, auxin, and BR; multiple hormones in signaling pathways interact and trigger downstream signaling cascades, leading to decreased cell cycle, cell wall biosynthesis and modification, and finally reduced internode length. In addition, MC slowed down secondary metabolism, such as lignin and flavonoid, in cotton internodes. Furthermore, the expression of many TFs such as bHLH, AP2-EREBP, Orphans, MYB, GRF, and TCP was altered by MC treatment, suggesting the important regulatory roles of TFs in internode elongation. Our findings suggest that multiple growth phytohormones (GA, auxin, and BR), secondary metabolism, and numerous TFs are involved in the MC-induced inhibition of internode elongation. This study was performed at the transcrioption level, further studies need to investigate the response to MC treatment at the protein level. Moreover, future studies are required to identify the function of the identified genes.

Methods

Plant materials and treatments

Gossypium hirsutum (CCRI49) seeds were obtained from Institute of Cotton Research of Chinese Academy of Agricultural Sciences (Anyang, China). Cotton seeds were immersed in water for 8 h at 37°C, and then germinated in sand at 28 °C in the dark for 3 days. Subsequently, uniform seedlings were transferred to plastic pots filled with aerated half-strength Hoagland solution and grown hydroponically in a growth chamber with a 14 h photoperiod at a 28/20 °C day/night temperature cycle, with a light intensity of 550 mmol m^{-2} s^{-1}.

Based on the findings of our previous study [37], we used 80 mg/L of MC for treatment in this study. The MC standard (purity, 97.0%) was supplied by Hebei Guoxin ahadzi-nonon Biological Technology Co., Ltd. (Hejian, Heibei, China). At the three-leaf stage, 120 seedlings were randomly divided into two groups: MC

(90 seedlings) and deionized water as control (30 seedlings). Both treatments were applied to the seedlings by foliar spray. The experiments were performed with three replicates. The length of each internode was measured at the tenth day after treatment. The length of the second internode, an elongating internode, was measured before plants were subjected to MC treatment, and then at 2-day intervals for 10 days. The second internodes were harvested at 0, 48, 72, and 96 h after treatment for RNA extraction and transcriptome analysis. The upper halves of the second internodes were sampled at the tenth day after treatment for endogenous hormone content and cell morphology analyses.

Histological analysis

Ten elongating second internodes were collected for the measurement of cell length and cell number of MC-treated and control plants 10 days after MC treatment. The upper zones of the internodes (approximately 5 mm each) were fixed in formalin–acetic acid–alcohol fluid containing 5 % acetic acid, 45 % ethanol, and 5 % formaldehyde. The samples were dehydrated in a graded ethanol/tert-butanol series, embedded in paraffin, and sectioned longitudinally to 10 μm on a rotary microtome (Leica Instruments GmbH; Wetzlar, Germany). Paraffin sections were stained with fast green and digitized using Pannoramic P250 Flash (3DHistech; Hungary). The length of about 100 cells per internode was measured from the longitudinal sections of cortex cells by using Caseviewer software 3.3 (3D HISTECH Ltd., Budapest, Hungary). The cell number in each internode was estimated as the ratio of internode length to mean cell length.

RNA extraction and transcriptome analysis

Total RNA was extracted from the second internodes by using RNAprep Pure Plant Kit (Tiangen, Beijing, China) and then treated with RNase-free DNase I (Takara) to remove genomic DNA. The RNA was electrophoresed on 1% agarose gels for monitoring RNA degradation and contamination. RNA purity, concentration, and integrity were further assessed using Nanodrop (Thermo Scientific, USA), Qubit (Life Technologies, CA, USA), and Agilent 2100 (Agilent Technologies, CA, USA). Twelve RNA-Seq libraries (4 time points × 3 biological replicates) were prepared using the Next Ultra Directional RNA Library Prep Kit (NEB), following manufacturer's instructions. In brief, mRNA was purified from total RNA by using poly-T oligo-attached magnetic beads. The mRNA was fragmented into small pieces by using a divalent cation under elevated temperature, and then first-strand cDNA was synthesized by using random hexamer primers and M-MuLV Reverse Transcriptase (NEB). Following cDNA synthesis, the second-strand cDNA was synthesized using DNA polymerase I and RNaseH. Subsequently, the cDNA fragments were adenylated and ligated with adaptors. The ligation products were purified and then enriched using PCR amplification to create libraries. RNA-Seq library sequencing was performed using an Illumina HiSeq4000 platform at Novogene Bioinformatics Institute (Beijing, China).

Transcriptome sequence processing and analysis

Raw sequencing data in FASTQ format were first filtered to remove adapter sequences and low-quality reads (reads with ambiguous bases, >10% and more than 50% bases with Q ≤ 20) to obtain clean reads

by using custom Perl scripts. The clean reads were mapped to the cotton reference genome (https://www.cottongen.org/species/Gossypium_hirsutum/nbi-AD1_genome) by using HISAT software program [101]. To quantify gene expression level, we calculated read counts by using HTSeq v0.5.4p3 and normalized to the FPKM value [102]. The DESeq package (ver. 2.1.0) was used for pairwise gene expression comparisons between treatment groups (48 vs. 0 h, 72 vs. 0 h, and 96 vs. 0 h) and control (0 h) [102]. The DEGs were identified using a FDR of ≤0.05; absolute value of log2 (fold change), ≥1; and more than 1 FPKM in at least one sample of each comparison.

GO and KEGG enrichment analysis

GO enrichment analysis of DEGs was performed using the GOseq R package [103], with corrected *P*-value of <0.05 regarded as significant. KEGG pathways analysis of the DEGs was performed using KOBAS software [104].

Quantitative real-time PCR analysis

The same total RNA samples used for transcriptome analysis were used for quantitative real-time PCR (qPCR) analysis. DNA-free total RNA (1 μg) was reverse transcribed into cDNA by using oligo (dT)20 primers and MMLV reverse transcriptase (Takara, Japan). The cDNAs were diluted 10-fold for qPCR analysis. Real-time PCR mixture (20 μL in total volume) included 10 μL of SYBR Premier Ex TaqII mix (Takara, Japan), 0.5 μL of each primer (10 μM), 2 μL of diluted cDNA, and 7 μL DNase-free water. qPCR was performed on a LightCycler 96 real-time PCR instrument (Roche, Switzerland), initiated at 95 °C for 10 min, followed by 45 cycles at 95 °C for 10 s and 60 °C for 30 s. Melting curve analysis was performed at 95 °C for 10 s, 65 °C for 60 s, and 97 °C for 1 s. *GhActin4* was used as an internal control to normalize the gene expression. All analyses were repeated twice by using three replicates. Primers used for qRT-PCR (Table S1) were designed using Primer3 software (http://primer3.sourceforge.net).

Hormone quantification

At 6 days after MC treatment, the second internode was used for the measurement of the content of endogenous GA_3, GA_4, IAA, trans-zeatin, and brassinolide. Endogenous GA_3 and GA_4 were extracted and quantified as previously described [37]. For the extraction of IAA and trans-zeatin, about 1 g of plant material was frozen in liquid nitrogen and ground into powder. Next, 10 mL of isopropanol-HCl buffer solution (2:0.002, v/v) was added to the powder and shaken for 30 min at 4 °C. Subsequently, dichloromethane (20 mL) was added, shaken for 30 min, and then centrifuged at 13 000 *g* for 5 min. After centrifugation, the lower organic phase was transferred to a 50 mL tube and evaporated in a constant stream of nitrogen. Each sample was kept in the dark and resolubilized in 400 μL methanol containing 0.1 % formic acid, and then filtered using a 0.22 μm microfilter for HPLC-MS/MS analysis. For brassinolide measurement, 2 g of plant material was homogenized in liquid nitrogen with 10 mL 80 % methanol and then incubated at 4 °C for 2 h in the dark. The homogenate was centrifuged at 10 000 *g* for 5 min at 4 °C. The supernatant was loaded onto a Bond Elut C18 column (ODS; Agilent Technologies, Santa Clara, CA USA) that was eluted with 80 % methanol. The eluate was further loaded onto strata-X

column that was eluted with 80 % methanol. The eluate solution was evaporated in a constant stream of nitrogen, re-dissolved in 200 mL methanol, and then filtered using a 0.22 μm microfilter for HPLC-MS/MS analysis. The experiments were repeated three times.

Statistical analysis

Data were the average of three independent sample measurements. Error bars indicate the standard deviation from the mean of biological triplicates. Statistical significance was evaluated using Student's *t*-test by using SPSS 17.0 software at 0.05 (*) or 0.01 (**) probability levels.

Abbreviations

4CL: 4-coumarate-CoA ligase; 4CLL: 4-coumarate-CoA ligase-like; ABA: Abscisic acid; ABAHs: ABA 8'-hydroxylases; ACC: 1-aminocyclopropane-1-carboxylate; ACO: ACC oxidase; ACS: ACC synthase; AGP: Arabinogalactan protein; AQPs: Aquaporins; BEE: BR-ENHANCED EXPRESSION; BL: Brassinolide; BR: Brassinosteroid; CAD: Cinnamyl alcohol dehydrogenase; CCR: Cinnamoyl-CoA reductase; CHS: Chalcone synthase; CK: Cytokinin; CKS1: Cyclin-dependent kinases regulatory subunit 1; CNR1: Cell number regulator 1; COMT: Caffeic acid 3-O-methyltransferase; CPS: Copalyl diphosphate synthase; CSE: Caffeoylshikimate esterase; CYC: Cyclin genes; CYP78A: Cytochrome P450 78A; DEGs: Differentially expressed genes; EXPA: Expansin; FDR: False discovery rate; FLAs: Fasciclin-like arabinogalactan proteins; FLS: Flavonol synthase; GA: Gibberellin; GA20ox2: GA 20 oxidase 2; GID1: GIBBERELLIN INSENSITIVE DWARF1; GO: Gene Ontology; HCT: Shikimate O-hydroxycinnamoyltransferase; JA: Jasmonic acid; KEGG: Kyoto Encyclopedia of Genes and Genomes; KRP: Cyclin-dependent kinase inhibitor; KS: Entcopalyl diphosphate synthase; LAC: Laccase; LDOX: Leucoanthocyanidin dioxygenase; LRX: Leucine-rich repeat extensin-like protein; MC: Mepiquat chloride; NCED3: 9-cis epoxy carotenoid dioxygenase 3; PAC: Paclobutrazol; PIPs: Plasma membrane intrinsic proteins; Pro-Ca: prohexadione-Ca; PRX: Peroxidase;; SA: Salicylic acid; SAM: S-adenosyl methionine; TFs: transcription factors; FPKM: Fragments Per Kb per Million of the mapped reads; TIPs: Tonoplast intrinsic proteins; XTHs: Xyloglucan endotransglycolase/hydrolases.

Declarations

Acknowledgements

We thank Junqiang Guo (Faculty of Information Engineering and Automation, Kunming University of Science and Technology) for excellent technical assistance.

Funding

This work was supported by the National Natural Science Foundation of China (Grant no. 31601241 and 31771703), and the Research Fund of the major program of Science and Technology in Henan Provincial Committee of Education (Grant no. 17A180007). The funding organizations provided the financial

support to the research projects, but didn't involved in study design, data collection, analysis, and in writing the manuscript.

Availability of data and materials

The sequencing data are deposited in NCBI Sequence Read Archive (SRA, http://www.ncbi.nlm.nih.gov/Traces/sra) with accession number PRJNA555146.

Authors' contributions

YL and LW conceived the idea and supervised the research. LW, YY and LFW grew cotton seedlings and performed MC treatment, samples collection and RNA extractions. YY and LFW performed histological analysis; LW, YY, LFW MW, MZ and YT performed DEG data analysis; YY and LFW performed qRT-PCR analyses. YL, LW wrote the manuscript. All authors read and approved the final manuscript.

Ethics approval and consent to participate

Not applicable.

Consent for publication

Not applicable.

Competing interests

The authors declare that they have no competing interests.

Publisher's Note

Springer Nature remains neutral with regard to jurisdictional claims in published maps and institutional affiliations.

Author details

College of Life Sciences, Henan Normal University, Xinxiang 453007, Henan, P. R. China.

References

1. Zhao D, Oosterhuis DM. Pix plus and mepiquat chloride effects on physiology, growth,and yield of field-grown cotton. J Plant Growth Regul. 2000;19(4):415-22.
2. Wang B, Smith SM, Li J. Genetic regulation of shoot architecture. Annu Rev Plant Biol. 2018;69(1):437-68.
3. Van De Velde K, Ruelens P, Geuten K, Rohde A, Van Der Straeten D. Exploiting DELLA signaling in cereals. Trends Plant Sci. 2017;22(10):880 - 93.

4. Fukazawa J, Mori M, Watanabe S, Miyamoto C, Ito T, Takahashi Y. DELLA-GAF1 Complex is a main component in gibberellin feedback regulation of GA20 oxidase 2. Plant Physiol. 2017;175(3):1395-406.
5. Rademacher W. GROWTH RETARDANTS: Effects on gibberellin biosynthesis and other metabolic pathways. Annu Rev Plant Physiol Plant Mol Biol. 2000;51(1):501-31.
6. Upreti KK, Reddy YTN, Prasad SRS, Bindu GV, Jayaram HL, Rajan S. Hormonal changes in response to paclobutrazol induced early flowering in mango cv. Totapuri Sci Hortic. 2013;150:414 - 18.
7. Liu Y, Fang Y, Huang M, Jin Y, Sun J, Tao X, Zhang G, He K, Zhao Y, Zhao H. Uniconazole-induced starch accumulation in the bioenergy crop duckweed (*Landoltia punctata*) II: transcriptome alterations of pathways involved in carbohydrate metabolism and endogenous hormone crosstalk. Biotechnol Biofuels. 2015;8(1):64.
8. Grossmann K, König-Kranz S, Kwiatkowski J. Phytohormonal changes in intact shoots of wheat and oilseed rape treated with the acylcyclohexanedione growth retardant prohexadione calcium. Physiol Plant. 1994;90(1):139-43.
9. Yokota T, Nakamura Y, Takahashi N, Nonaka M, Sekimoto H, Oshio H, Takatsuto S. Inconsistency between growth and endogenous levels of gibberellins, brassinosteroids, and sterols in Pisum Sativum treated with uniconazole antipodes. Gibberellins. 1991;339-49.
10. Kraus TE, Murr DP, Hofstra G, Fletcher RA. Modulation of ethylene synthesis in acotyledonous soybean and wheat seedlings. J Plant Growth Regul. 1992;11(1):47.
11. Min XJ, Bartholomew DP. Effect of plant growth regulators on ethylene production, 1-aminocyclopropane-1-carboxylic acid oxidase activity, and initiation of inflorescence development of pineapple. J Plant Growth Regul. 1996;15(3):121.
12. Seesangboon A, Gruneck L, Pokawattana T, Eungwanichayapant PD, Tovaranonte J, Popluechai S. Transcriptome analysis of *Jatropha curcas* L. flower buds responded to the paclobutrazol treatment. Plant Physiol Biochem. 2018;127:276 - 86.
13. Zhang D, Ren L, Yue JH, Shi YB, Zhuo LH, Wang L, Shen XH. RNA-Seq-based transcriptome analysis of stem development and dwarfing regulation in *Agapanthus praecox* ssp. *orientalis* (Leighton) Leighton. Gene. 2015; 565(2):252 - 67.
14. Marowa P, Ding A, Kong Y. Expansins: roles in plant growth and potential applications in crop improvement. Plant Cell Rep. 2016;35(5):949-65.
15. Minami A, Yano K, Gamuyao R, Nagai K, Kuroha T, Ayano M, Nakamori M, Koike M, Kondo Y, Niimi Y, Kuwata K, Suzuki T, Higashiyama T, Takebayashi Y, Kojima M, Sakakibara H, Toyoda A, Fujiyama A, Kurata N, Ashikari M, Reuscher S. Time-course transcriptomics analysis reveals key responses of submerged deepwater rice to flooding. Plant Physiol. 2018; 176(4):3081-102.
16. Dare AP, Tomes S, Jones M, McGhie TK, Stevenson DE, Johnson RA, Greenwood DR, Hellens RP. Phenotypic changes associated with RNA interference silencing of chalcone synthase in apple (*Malus* × *domestica*). Plant J. 2013;74(3):398-410.

17. Muro-Villanueva F, Mao X, Chapple C. Linking phenylpropanoid metabolism, lignin deposition, and plant growth inhibition. Curr Opin Biotechnol. 2019;56:202 - 08.
18. Davière JM, Wild M, Regnault T, Baumberger N, Eisler H, Genschik P, Achard P. Class I TCP-DELLA interactions in inflorescence shoot apex determine plant height. Curr Biol. 2014;24(16):1923 - 28.
19. Kuijt SJ, Greco R, Agalou A, Shao J, 't Hoen CC, Overnäs E, Osnato M, Curiale S, Meynard D, van Gulik R, de Faria Maraschin S, Atallah M, de Kam RJ, Lamers GE, Guiderdoni E, Rossini L, Meijer AH, Ouwerkerk PB. Interaction between the GROWTH-REGULATING FACTOR and KNOTTED1-LIKE HOMEOBOX families of transcription factors. Plant Physiol. 2014; 164(4):1952-66.
20. Wolf S. Plant cell wall signalling and receptor-like kinases. Biochem J. 2017;474(4):471-92.
21. Pien S, Wyrzykowska J, McQueen-Mason S, Smart C, Fleming A. Local expression of expansin induces the entire process of leaf development and modifies leaf shape. Proc Natl Acad Sci. 2001;98(20):11812-17.
22. Tan J, Tu L, Deng F, Hu H, Nie Y, Zhang X. A genetic and metabolic analysis revealed that cotton fiber cell development was retarded by flavonoid naringenin. Plant Physiol. 2013;162(1):86-95.
23. Pollak PE, Hansen K, Astwood JD, Taylor LP. Conditional male fertility in maize. Sex Plant Reprod. 1995;8(4):231-41.
24. Schijlen EG, de Vos CH, Martens S, Jonker HH, Rosin FM, Molthoff JW, Tikunov YM, Angenent GC, van Tunen AJ, Bovy AG. RNA interference silencing of chalcone synthase, the first step in the flavonoid biosynthesis pathway, leads to parthenocarpic tomato fruits. Plant Physiol. 2007;144(3):1520-30.
25. Leplé JC, Dauwe R, Morreel K, Storme V, Lapierre C, Pollet B, Naumann A, Kang KY, Kim H, Ruel K, Lefèbvre A, Joseleau JP, Grima-Pettenati J, De Rycke R, Andersson-Gunnerås S, Erban A, Fehrle I, Petit-Conil M, Kopka J, Polle A, Messens E, Sundberg B, Mansfield SD, Ralph J, Pilate G, Boerjan W. Downregulation of cinnamoyl-coenzyme A reductase in poplar: multiple-level phenotyping reveals effects on cell wall polymer metabolism and structure. Plant cell. 2007;19(11):3669-91.
26. Pinçon G, Maury S, Hoffmann L, Geoffroy P, Lapierre C, Pollet B, Legrand M. Repression of O-methyltransferase genes in transgenic tobacco affects lignin synthesis and plant growth. Phytochemistry. 2001;57(7):1167 - 76.
27. Shadle G, Chen F, Srinivasa Reddy MS, Jackson L, Nakashima J, Dixon RA. Down-regulation of hydroxycinnamoyl CoA: shikimate hydroxycinnamoyl transferase in transgenic alfalfa affects lignification, development and forage quality. Phytochemistry. 2007;68(11):1521 - 29.
28. Martín-Trillo M, Cubas P. TCP genes: a family snapshot ten years later. Trends Plant Sci. 2010;15(1):31 - 39.
29. Zhou H, Song X, Wei K, Zhao Y, Jiang C, Wang J, Tang F, Lu M. Growth-regulating factor 15 is required for leaf size control in Populus. Tree Physiol. 2019;39(3):381-90.
30. Davière JM, Achard P. A pivotal role of DELLAs in regulating multiple hormone signals. Mol Plant. 2016;9(1):10 - 20.

31. Zhiponova MK, Morohashi K, Vanhoutte I, Machemer-Noonan K, Revalska M, Van Montagu M, Grotewold E, Russinova E. Helix–loop–helix/basic helix–loop–helix transcription factor network represses cell elongation in Arabidopsis through an apparent incoherent feed-forward loop. Proc Natl Acad Sci U S A. 2014;111(7):2824-29.
32. Rosolem CA, Oosterhuis DM, Souza FS. Cotton response to mepiquat chloride and temperature. Sci agric. 2013;70:82-87.
33. Siebert JD, Stewart AM. Influence of plant density on cotton response to mepiquat chloride application. Agron J. 2006;98(6):1634-39.
34. Ren X, Zhang L, Du M, Evers JB, Wopke VDW, Tian X, Li Z. Managing mepiquat chloride and plant density for optimal yield and quality of cotton. Field Crops Res. 2013;149:1-10.
35. Reddy VR, Baker DN, Hodges HF. Temperature and mepiquat chloride effects on cotton canopy architecture. Agron J. 1990;82(2):190-95.
36. Shechter I, West CA. Biosynthesis of gibberellins: IV. Biosynthesis of cyclic diterpenes from trans-geranylgeranyl pyrophosphate. J Biol Chem. 1969;244(12):3200-09.
37. Wang L, Mu C, Du M, Chen Y, Tian X, Zhang M, Li Z. The effect of mepiquat chloride on elongation of cotton (*Gossypium hirsutum* L.) internode is associated with low concentration of gibberellic acid. Plant Sci. 2014;225:15 - 23.
38. Ding L, Uehlein N, Kaldenhoff R, Guo S, Zhu Y, Kai L. Aquaporin PIP2;1 affects water transport and root growth in rice (*Oryza sativa* L.). Plant Physiol Biochem. 2019;139:152 - 60.
39. Li G, Santoni, Véronique, Maurel C. Plant aquaporins: roles in plant physiology. Biochim Biophys Acta Gen Subj. 2014;1840(5):1574 - 82.
40. Adams S, Grundy J, Veflingstad SR, Dyer NP, Hannah MA, Ott S, Carré IA. Circadian control of abscisic acid biosynthesis and signalling pathways revealed by genome-wide analysis of LHY binding targets. New Phytol. 2018;220(3):893-907.
41. Ni J, Shah FA, Liu W, Wang Q, Wang D, Zhao W, Lu W, Huang S, Fu S, Wu L. Comparative transcriptome analysis reveals the regulatory networks of cytokinin in promoting the floral feminization in the oil plant *Sapium sebiferum*. BMC Plant Biol. 2018;18(1):96.
42. Friedrichsen DM, Nemhauser J, Muramitsu T, Maloof JN, Alonso J, Ecker JR, Furuya M,Chory J. Three redundant brassinosteroid early response genes encode putative bHLH transcription factors required for normal growth. Genetics. 2002;162(3):1445-56.
43. York AC. Cotton cultivar response to mepiquat chloride. Agron J. 1983;75(4):663-67.
44. Sablowski R, Carnier Dornelas M. Interplay between cell growth and cell cycle in plants. J Exp Bot. 2014;65(10):2703-14.
45. Baek GH, Kim I, Rao H. The Cdc48 ATPase modulates the interaction between two proteolytic factors Ufd2 and Rad23. Proc Natl Acad Sci U S A. 2011;108(33):13558-63.
46. Adamski NM, Anastasiou E, Eriksson S, O'Neill CM, Lenhard M. Local maternal control of seed size by KLUH/CYP78A5-dependent growth signaling. Proc Natl Acad Sci U S A. 2009;106(47):20115-20.

47. Fang W, Wang Z, Cui R, Li J, Li Y. Maternal control of seed size by *EOD3*/*CYP78A6* in *Arabidopsis thaliana*. Plant J. 2012;70(6):929-39.
48. Ma M, Wang Q, Li Z, Cheng H, Li Z, Liu X, Song W, Appels R, Zhao H. Expression of *TaCYP78A3*, a gene encoding cytochrome P450 CYP78A3 protein in wheat (*Triticum aestivum* L.), affects seed size. Plant J. 2015;83(2):312-25.
49. Ma M, Zhao H, Li Z, Hu S, Song W, Liu X. *TaCYP78A5* regulates seed size in wheat (*Triticum aestivum*). J Exp Bot. 2016;67(5):1397-410.
50. Guo M, Rupe MA, Dieter JA, Zou J, Spielbauer D, Duncan KE, Howard RJ, Hou Z, Simmons CR. Cell Number Regulator1 affects plant and organ size in maize: implications for crop yield enhancement and heterosis. Plant cell. 2010;22(4):1057-73.
51. Atkinson RG, Johnston SL, Yauk YK, Sharma NN, Schröder R. Analysis of xyloglucan endotransglucosylase/hydrolase (XTH) gene families in kiwifruit and apple. Postharvest Biol Technol. 2009;51(2):149 - 57.
52. Jeong HY, Nguyen HP, Lee C. Genome-wide identification and expression analysis of rice pectin methylesterases: Implication of functional roles of pectin modification in rice physiology. J Plant Physiol. 2015;183:23 - 29.
53. Yang Z, Zhang C, Yang X, Liu K, Wu Z, Zhang X, Zheng W, Xun Q, Liu C, Lu L, Yang Z, Qian Y, Xu Z, Li C, Li J, Li F. PAG1, a cotton brassinosteroid catabolism gene, modulates fiber elongation. New Phytol. 2014;203(2):437-48.
54. Coll-Garcia D, Mazuch J, Altmann T, Müssig C. EXORDIUM regulates brassinosteroid-responsive genes. FEBS Lett. 2004;563(1-3):82-86.
55. Shi H, Kim Y, Guo Y, Stevenson B, Zhu JK. The Arabidopsis *SOS5* locus encodes a putative cell surface adhesion protein and is required for normal cell expansion. Plant cell. 2003;15(1):19-32.
56. Huang GQ, Gong SY, Xu WL, Li W, Li P, Zhang CJ, Li DD, Zheng Y, Li FG, Li XB. A fasciclin-like arabinogalactan protein, GhFLA1, is involved in fiber initiation and elongation of cotton. Plant Physiol. 2013;161(3):1278-90.
57. Chaumont F, Tyerman SD. Aquaporins: highly regulated channels controlling plant water relations. Plant Physiol. 2014;164(4):1600-18.
58. Phillips AL, Huttly AK. Cloning of two gibberellin-regulated cDNAs from Arabidopsis thaliana by subtractive hybridization: expression of the tonoplast water channel, gamma-TIP, is increased by GA3. Plant Mol Biol. 1994;24(4):603-15.
59. Péret B, Li G, Zhao J, Band LR, Voß U, Postaire O, Luu DT, Da Ines O, Casimiro I, Lucas M, Wells DM, Lazzerini L, Nacry P, King JR, Jensen OE, Schäffner AR, Maurel C, Bennett MJ. Auxin regulates aquaporin function to facilitate lateral root emergence. Nat Cell Biol. 2012;14:991.
60. Ma N, Xue J, Li Y, Liu X, Dai F, Jia W, Luo Y, Gao J. *Rh-PIP2;1*, a rose aquaporin gene, is involved in ethylene-regulated petal expansion. Plant Physiol. 2008;148(2):894-907.
61. Wang F, Zhu D, Huang X, Li S, Gong Y, Yao Q, Fu X, Fan LM, Deng XW. Biochemical insights on degradation of Arabidopsis DELLA proteins gained from a cell-free assay system. Plant cell.

2009;21(8):2378-90.

62. Tao Y, Ferrer JL, Ljung K, Pojer F, Hong F, Long JA, Li L, Moreno JE, Bowman ME, Ivans LJ, Cheng Y, Lim J, Zhao Y, Ballaré CL, Sandberg G, Noel JP, Chory J. Rapid synthesis of auxin via a new tryptophan-dependent pathway is required for shade avoidance in plants. Cell. 2008;133(1):164 - 76.
63. Staswick PE, Serban B, Rowe M, Tiryaki I, Maldonado MT, Maldonado MC, Suza W. Characterization of an Arabidopsis enzyme family that conjugates amino acids to indole-3-acetic acid. Plant cell. 2005;17(2):616-27.
64. Björklund S, Antti H, Uddestrand I, Moritz T, Sundberg B. Cross-talk between gibberellin and auxin in development of *Populus* wood: gibberellin stimulates polar auxin transport and has a common transcriptome with auxin. Plant J. 2007;52(3):499-511.
65. Moubayidin L, Perilli S, Dello Ioio R, Di Mambro R, Costantino P, Sabatini S. The rate of cell differentiation controls the Arabidopsis root meristem growth phase. Curr Biol. 2010; 20(12):1138 - 43.
66. Ohnishi T, Szatmari AM, Watanabe B, Fujita S, Bancos S, Koncz C, Lafos M, Shibata K, Yokota T, Sakata K, Szekeres M, Mizutani M. C-23 hydroxylation by *Arabidopsis* CYP90C1 and CYP90D1 reveals a novel shortcut in brassinosteroid biosynthesis. Plant cell. 2006;18(11):3275-88.
67. Postel S, Küfner I, Beuter C, Mazzotta S, Schwedt A, Borlotti A, Halter T, Kemmerling B, Nürnberger T. The multifunctional leucine-rich repeat receptor kinase BAK1 is implicated in *Arabidopsis* development and immunity. Eur J Cell Biol. 2010;89(2):169 - 74.
68. Noh SA, Choi YI, Cho JS, Lee H. The poplar basic helix-loop-helix transcription factor BEE3 -Like gene affects biomass production by enhancing proliferation of xylem cells in poplar. Biochem Biophys Res Commun. 2015;462(1):64 - 70.
69. Weiss D, Ori N. Mechanisms of cross talk between gibberellin and other hormones. Plant Physiol. 2007;144(3):1240-46.
70. Kieber JJ,Schaller GE. Cytokinin signaling in plant development. Development. 2018; 145(4):dev149344.
71. Zeng XF, Zhao DG. Expression of *IPT* in *Asakura-sanshoo* (Zanthoxylum piperitum (L.) DC. f. *inerme Makino*) alters tree architecture, delays leaf senescence, and changes leaf essential oil composition. Plant Mol Biol Report. 2016;34(3):649-58.
72. Shi YH, Zhu SW, Mao XZ, Feng JX, Qin YM, Zhang L, Cheng J, Wei LP, Wang ZY, Zhu YX. Transcriptome profiling, molecular biological, and physiological studies reveal a major role for ethylene in cotton fiber cell elongation. Plant cell. 2006;18(3):651-64.
73. Van de Poel B, Smet D, Van Der Straeten D. Ethylene and hormonal cross talk in vegetative growth and development. Plant Physiol. 2015;169(1):61-72.
74. TakashiHirayama, KazuoShinozaki. Perception and transduction of abscisic acid signals: keys to the function of the versatile plant hormone ABA. Trends Plant Sci. 2007;12(8):343 - 51.
75. Xiao G, Zhao P, Zhang Y. A Pivotal role of hormones in regulating cotton fiber development. Front Plant Sci. 2019;10:87-87.

76. Lim S, Park J, Lee N, Jeong J, Toh S, Watanabe A, Kim J, Kang H, Kim DH, Kawakami N, Choi G. ABA-insensitive3, ABA-insensitive5, and DELLAs interact to activate the expression of *SOMNUS* and other high-temperature-inducible genes in imbibed seeds in *Arabidopsis*. Plant cell. 2013;25(12):4863-78.
77. Lee S, Lee S, Yang KY, Kim YM, Park SY, Kim SY, Soh MS. Overexpression of *PRE1* and its homologous genes activates gibberellin-dependent responses in Arabidopsis thaliana. Plant Cell Physiol. 2006;47(5):591-600.
78. Mizukami Y, Fischer RL. Plant organ size control: AINTEGUMENTA regulates growth and cell numbers during organogenesis. Proc Natl Acad Sci U S A. 2000;97(2):942-47.
79. Krizek BA, Bequette CJ, Xu K, Blakley IC, Fu ZQ, Stratmann JW, Loraine AE. RNA-Seq links the transcription factors AINTEGUMENTA and AINTEGUMENTA-LIKE6 to cell wall remodeling and plant defense pathways. Plant Physiol. 2016;171(3):2069-84.
80. Wang CQ, Sarmast MK, Jiang J, Dehesh K. The transcriptional regulator BBX19 promotes hypocotyl growth by facilitating COP1-Mediated EARLY FLOWERING3 degradation in Arabidopsis. Plant cell. 2015;27(4):1128-39.
81. Crocco CD, Locascio A, Escudero CM, Alabadí D, Blázquez MA, Botto JF. The transcriptional regulator BBX24 impairs DELLA activity to promote shade avoidance in *Arabidopsis thaliana*. Nat Commun. 2015;6:6202.
82. Holtan HE, Bandong S, Marion CM, Adam L, Tiwari S, Shen Y, Maloof JN, Maszle DR, Ohto MA, Preuss S, Meister R, Petracek M, Repetti PP, Reuber TL, Ratcliffe OJ, Khanna R. BBX32, an Arabidopsis B-Box protein, functions in light signaling by suppressing HY5-regulated gene expression and interacting with STH2/BBX21. Plant Physiol. 2011;156(4):2109-23.
83. Preuss SB, Meister R, Xu Q, Urwin CP, Tripodi FA, Screen SE, Anil VS, Zhu S, Morrell JA, Liu G, Ratcliffe OJ, Reuber TL, Khanna R, Goldman BS, Bell E, Ziegler TE, McClerren AL, Ruff TG, Petracek ME. Expression of the *Arabidopsis thaliana* BBX32 gene in soybean increases grain yield. PLoS One. 2012;7(2):e30717.
84. Edwards KD, Takata N, Johansson M, Jurca M, Novák O, Hényková E, Liverani S, Kozarewa I, Strnad M, Millar AJ, Ljung K, Eriksson ME. Circadian clock components control daily growth activities by modulating cytokinin levels and cell division-associated gene expression in *Populus* trees. Plant Cell Environ. 2018;41(6):1468-82.
85. Kim JH, Tsukaya H. Regulation of plant growth and development by the GROWTH-REGULATING FACTOR and GRF-INTERACTING FACTOR duo. J Exp Bot. 2015;66(20):6093-107.
86. Omidbakhshfard MA, Proost S, Fujikura U, Mueller-Roeber B. Growth-Regulating Factors (GRFs): a small transcription factor family with important functions in plant biology. Mol Plant. 2015;8(7):998 - 1010.
87. Kim JH, Choi D, Kende H. The AtGRF family of putative transcription factors is involved in leaf and cotyledon growth in *Arabidopsis*. Plant J. 2003;36(1):94-104.
88. Nelissen H, Eeckhout D, Demuynck K, Persiau G, Walton A, van Bel M, Vervoort M, Candaele J, De Block J, Aesaert S, Van Lijsebettens M, Goormachtig S, Vandepoele K, Van Leene J, Muszynski M,

Gevaert K, Inzé D, De Jaeger G. Dynamic changes in ANGUSTIFOLIA3 complex composition reveal a growth regulatory mechanism in the maize leaf. Plant cell. 2015; 27(6):1605-19.

89. Li S, Tian Y, Wu K, Ye Y, Yu J, Zhang J, Liu Q, Hu M, Li H, Tong Y, Harberd NP, Fu X. Modulating plant growth–metabolism coordination for sustainable agriculture. Nature. 2018;560(7720):595-600.
90. Li C1, Potuschak T, Colón-Carmona A, Gutiérrez RA, Doerner P. Arabidopsis TCP20 links regulation of growth and cell division control pathways. Proc Natl Acad Sci U S A. 2005;102(36):12978-83.
91. Kieffer M, Master V, Waites R, Davies B. TCP14 and TCP15 affect internode length and leaf shape in Arabidopsis.Plant J. 2011;68(1):147-58.
92. Challa KR, Aggarwal P, Nath U. Activation of *YUCCA5* by the transcription factor TCP4 integrates developmental and environmental signals to promote hypocotyl elongation in Arabidopsis. Plant cell. 2016;28(9):2117-30.
93. Vanholme R, Cesarino, Rataj K, Xiao Y, Sundin L, Goeminne G, Kim H, Cross J, Morreel K, Araujo P, Welsh L, Haustraete J, McClellan C, Vanholme B, Ralph J, Simpson GG, Halpin C, Boerjan W. Caffeoyl shikimate esterase (CSE) is an enzyme in the lignin biosynthetic pathway in *Arabidopsis*. Science. 2013;341(6150):1103-06.
94. Ha CM, Escamilla-Trevino L, Yarce JC, Kim H, Ralph J, Chen F, Dixon RA. An essential role of caffeoyl shikimate esterase in monolignol biosynthesis in *Medicago truncatula*. Plant J. 2016; 86(5):363-75.
95. Hoffmann L, Besseau S, Geoffroy P, Ritzenthaler C, Meyer D, Lapierre C, Pollet B, Legrand M. Silencing of hydroxycinnamoyl-coenzyme A shikimate/quinate hydroxycinnamoyltransferase affects phenylpropanoid biosynthesis. Plant cell. 2004;16(6):1446-65.
96. Meents MJ, Watanabe Y, Samuels AL. The cell biology of secondary cell wall biosynthesis. Ann Bot. 2018;121(6):1107-25.
97. Zhao Q, Nakashima J, Chen F, Yin Y, Fu C, Yun J, Shao H, Wang X, Wang ZY, Dixon RA. Laccase is necessary and nonredundant with peroxidase for lignin polymerization during vascular development in *Arabidopsis*. Plant cell. 2013;25(10):3976-87.
98. Biemelt S, Tschiersch H, Sonnewald U. Impact of altered gibberellin metabolism on biomass accumulation, lignin biosynthesis, and photosynthesis in transgenic tobacco plants. Plant Physiol. 2004;135(1):254-65.
99. Zhao XY, Zhu DF, Zhou B, Peng WS, Lin JZ, Huang XQ, He RQ, Zhuo YH, Peng D, Tang DY, Li MF, Liu XM. Over-expression of the *AtGA2ox8* gene decreases the biomass accumulation and lignification in rapeseed (*Brassica napus* L.). J Zhejiang Univ Sci B. 2010;11(7):471-81.
100. Brown DE, Rashotte AM, Murphy AS, Normanly J, Tague BW, Peer WA, Taiz L, Muday GK. Flavonoids act as negative regulators of auxin transport in vivo in arabidopsis. Plant Physiol. 2001;126(2):524-35.
101. Kim D, Langmead B, Salzberg SL. HISAT: a fast spliced aligner with low memory requirements. Nat Methods. 2015;12(4):357-60.
102. Anders S, Huber W. Differential expression analysis for sequence count data. Genome Biol. 2010;11(10):R106.

103. Young MD, Wakefield MJ, Smyth GK, Oshlack A. Gene ontology analysis for RNA-seq: accounting for selection bias. Genome Biol. 2010;11(2):R14.

104. Xie C, Mao X, Huang J, Ding Y, Wu J, Dong S, Kong L, Gao G, Li CY, Wei L. KOBAS 2.0: a web server for annotation and identification of enriched pathways and diseases. Nucleic Acids Res. 2011;39(Web Se erverissue):W316-22.

Table

Table 1 Summary of sequenced reads and mapping results of RNA-Seq libraries

mple ıme[a]	Raw reads	Clean reads	Q30 (%)	GC content (%)	Total mapped	Multiple mapped	Uniquely mapped
h -1	67855394	64904972	93.2	43.9	61507264 (94.8%)	4865201 (7.5%)	56642063 (87.3%)
h -2	73708010	71773542	93.8	43.3	69032402 (96.2%)	5062153 (7.1%)	63970249 (89.1%)
h -3	75369532	73516426	93.8	43.6	70106706 (95.4%)	5307252 (7.2%)	64799454 (88.1%)
;h -1	73297526	71221868	93.8	43.7	68271995 (95.9%)	5222539 (7.3%)	63049456 (88.5%)
;h -2	78997068	76151270	94.2	43.6	72804908 (95.6%)	5960774 (7.8%)	66844134 (87.8%)
;h -3	78116322	76378038	93.9	43.1	72961097 (95.5%)	5051227 (6.6%)	67909870 (88.9%)
:h -1	75917610	73986066	94.2	43.3	71032308 (96.0%)	5449090 (7.4%)	65583218 (88.6%)
:h -2	74496274	72546812	93.9	43.4	69372478 (95.6%)	5039603 (7.0%)	64332875 (88.7%)
:h -3	74790936	72704568	94.1	43.4	69631233 (95.8%)	5458006 (7.5%)	64173227 (88.3%)
;h -1	74650012	72340374	93.9	43.2	69382034 (95.9%)	5277424 (7.3%)	64104610 (88.6%)
;h -2	72959828	70537494	94.2	43.2	67509097 (95.7%)	5280269 (7.5%)	62228828 (88.2%)
;h -3	70121270	68244724	93.9	43.3	65098235 (95.4%)	4732830 (6.9%)	60365405 (88.5%)

a 0 h represents control; 48 h, 72 h and 96 h represent 48 h, 72 h and 96 h after mepiquat chloride treatment, respectively. Number 1, 2 and 3 at the end of the sample name represent three biological replicates.

Additional Files

Additional file 1: Figure S1. Pearson correlation between sample replicates. C0 means control, C48, C72 and C96 mean 48 h, 72 h and 96 h after mepiquat chloride (MC) treatment. 1, 2 and 3 represent three replicates.

Additional file 2: Figure S2. GO terms enrichment of MC-responsive genes in the second internode at different treatment time points. GO terms were annotated according to the biological process, cellular

component and molecular function, respectively.

Additional file 3: Table S1. KEGG pathways enriched for DEGs at different time points after MC treatment (48 h, 72 h and 96 h vs. the control (0 h)).

Additional file 4: Table S2. Expression of DEGs related to cell cycle and cell division in the second internode of cotton seedlings in response to MC.

Additional file 5: Table S3. Expression of DEGs related to cell wall biosynthesis and modification in the second internode of cotton seedlings in response to MC.

Additional file 6: Table S4. Expression of MC responsive aquaporin genes in the second internode of cotton seedlings.

Additional file 7: Table S5. Expression of DEGs involved in phytohormone metabolism, transport and signal transduction pathways in the second internode of cotton seedlings in response to MC.

Additional file 8: Table S6. Expression of DEGs involved in lignin and flavonoid metabolism pathway in the second internode of cotton seedlings in response to MC.

Additional file 9: Table S7. Expression of differentially expressed transcription factors in the second internode of cotton seedlings in response to MC.

Additional file 10: Table S8. Sequence of primers used for qRT-PCR assays in this study.

Figures

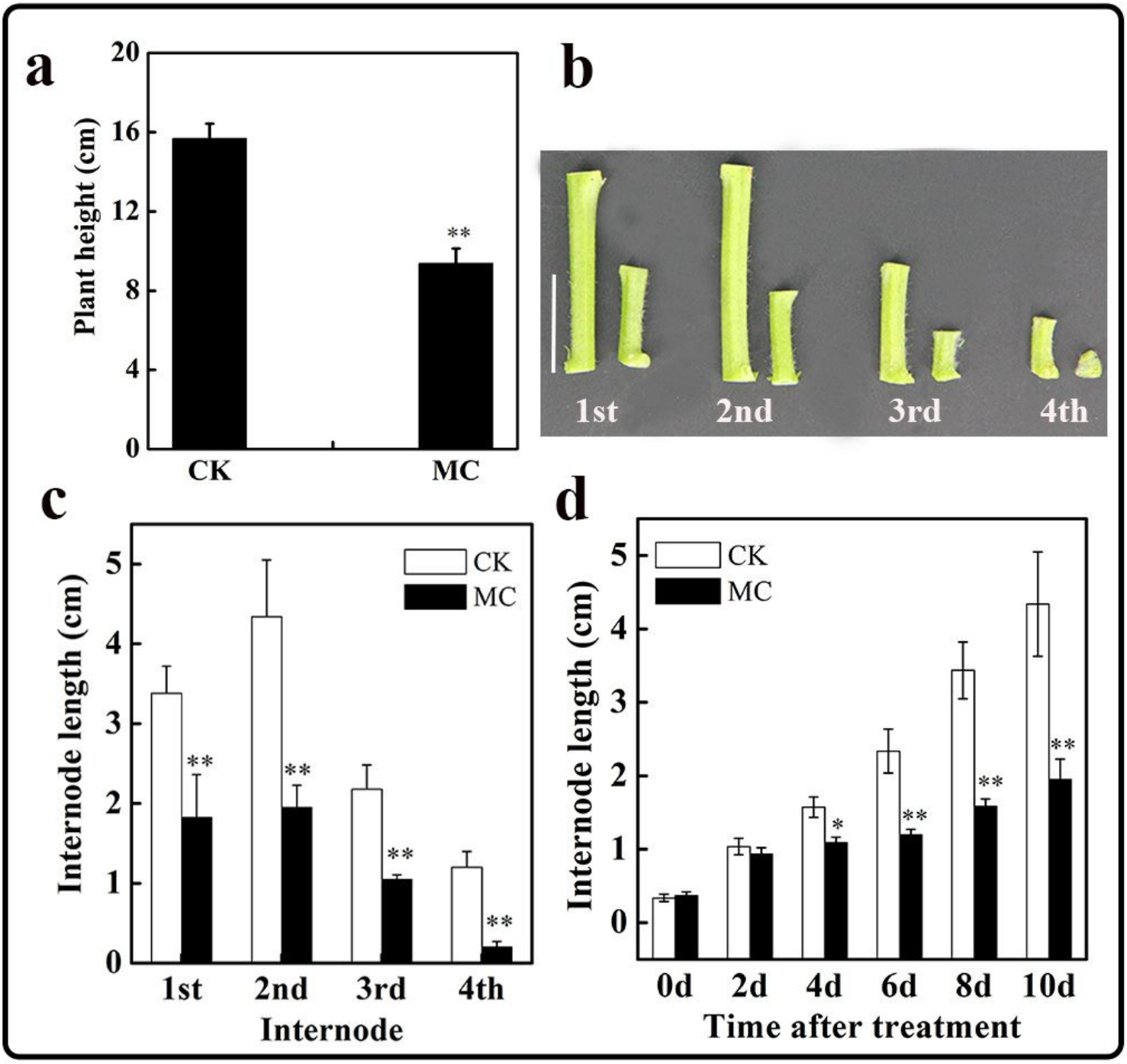

Figure 1

Effects of mepiquat chloride (MC) on plant height and internode length. (a) Plant height, (b) internode phenotype and (c) internode length of the control (CK) and MC-treated cotton seedlings at the tenth day after MC treatment. (d) Dynamic changes in the second internode length of cotton seedlings after MC treatment. Scale bars, 2 cm, *P < 0.05, **P < 0.01, Student's t-test.

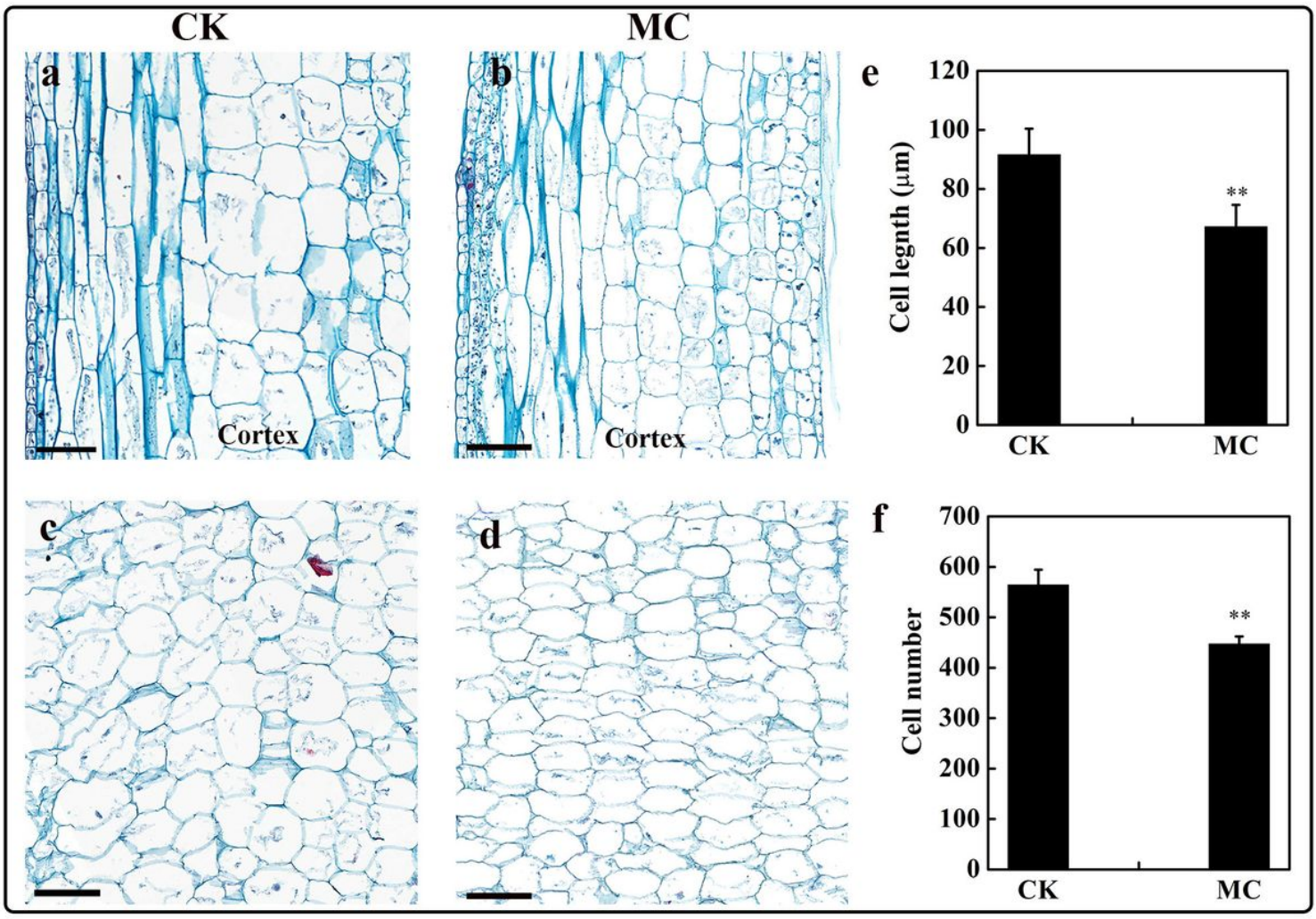

Figure 2

Histological observation of the second internode cells of cotton seedlings at the tenth day after MC treatment. (a, c) Cortex and pith cells from the second internode of control plants, respectively. (b, d) Cortex and pith cells from the second internode of MC-treated plants, respectively. (e, f) Cell length and cell number from the cortex of the second internode, respectively. All scale bars, 100 μm, **P < 0.01, Student's t-test.

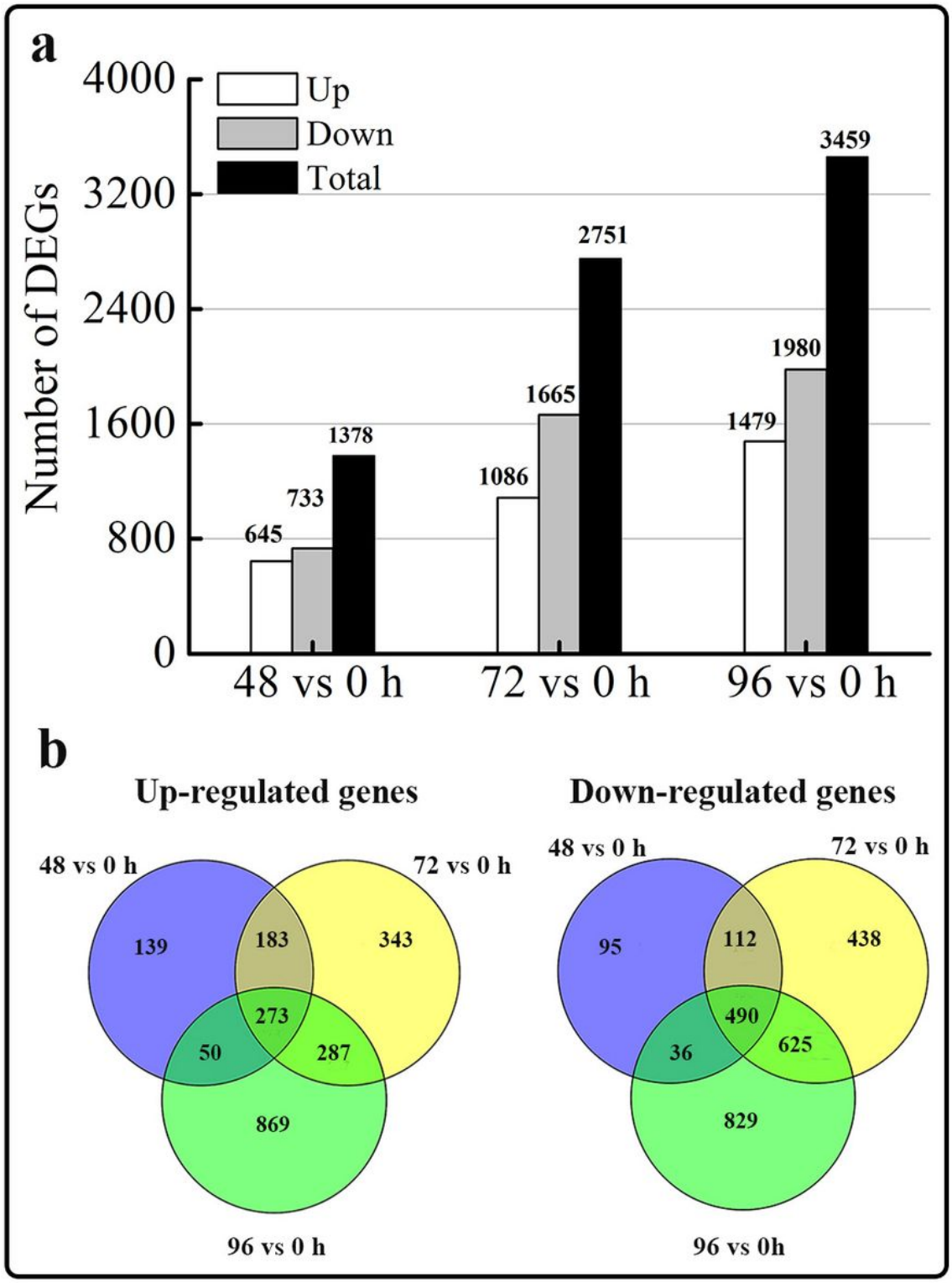

Figure 3

Differentially expression genes (DEGs) analysis. (a) Number of DEGs responding to MC-treatment (48 h, 72 h, 96 h vs. 0 h). (b) Venn diagram of DEGs at different time point after MC treatment.

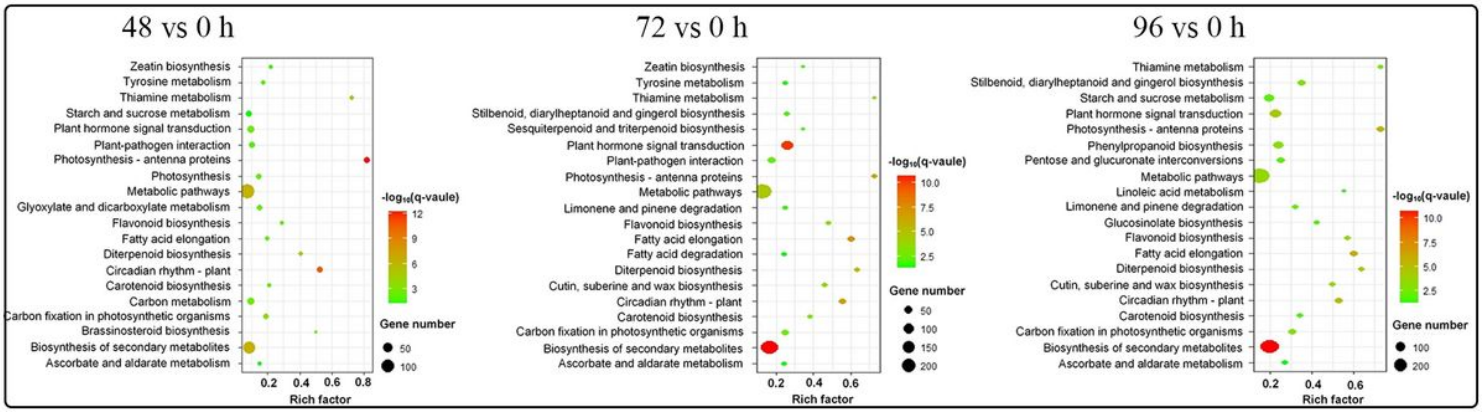

Figure 4

KEGG pathway enrichment analysis of DEGs between MC treatment and control. Y-axis shows the KEGG pathway. X-axis shows the Rich factor. The enrichment factor indicates the ratio of differentially expression genes enriched in this pathway to the total number of annotated genes. The size and color of each point represents the number of genes enriched in a particular pathway and the -log10 (q-value), respectively, 0 h: Control; 48, 72 and 96: 48 h, 72 h and 96 h after MC-treatment.

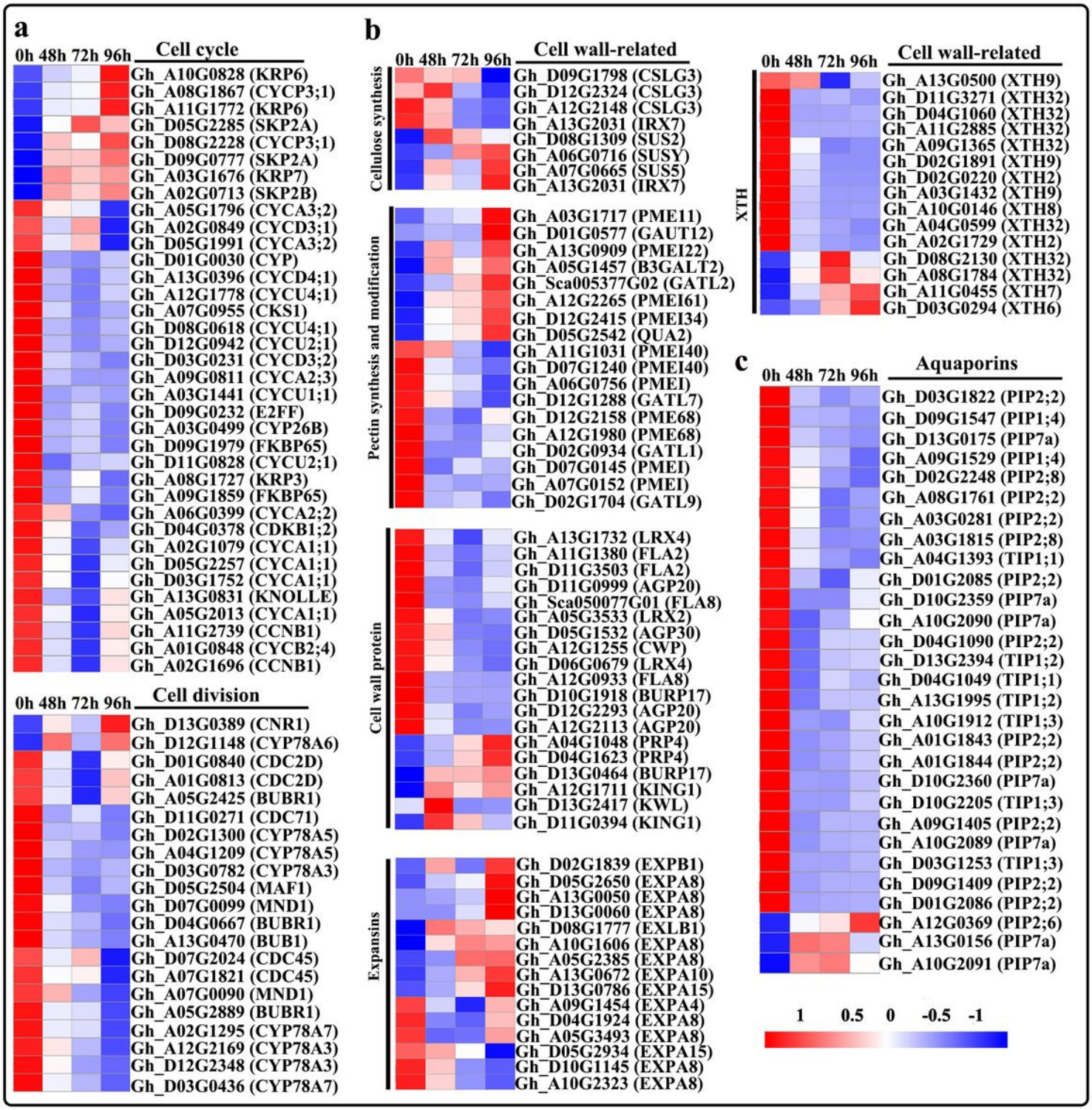

Figure 5

Heatmap of differentially expressed genes involved in plant hormone biosynthesis, transport, and signaling transduction in the second internode between MC treatment and control. Gene expression level (FPKM) was normalized with Z-score. Blue indicates lower expression, and red indicates higher expression. 0 h: Control; 48, 72 and 96: 48 h, 72 h and 96 h after MC-treatment.

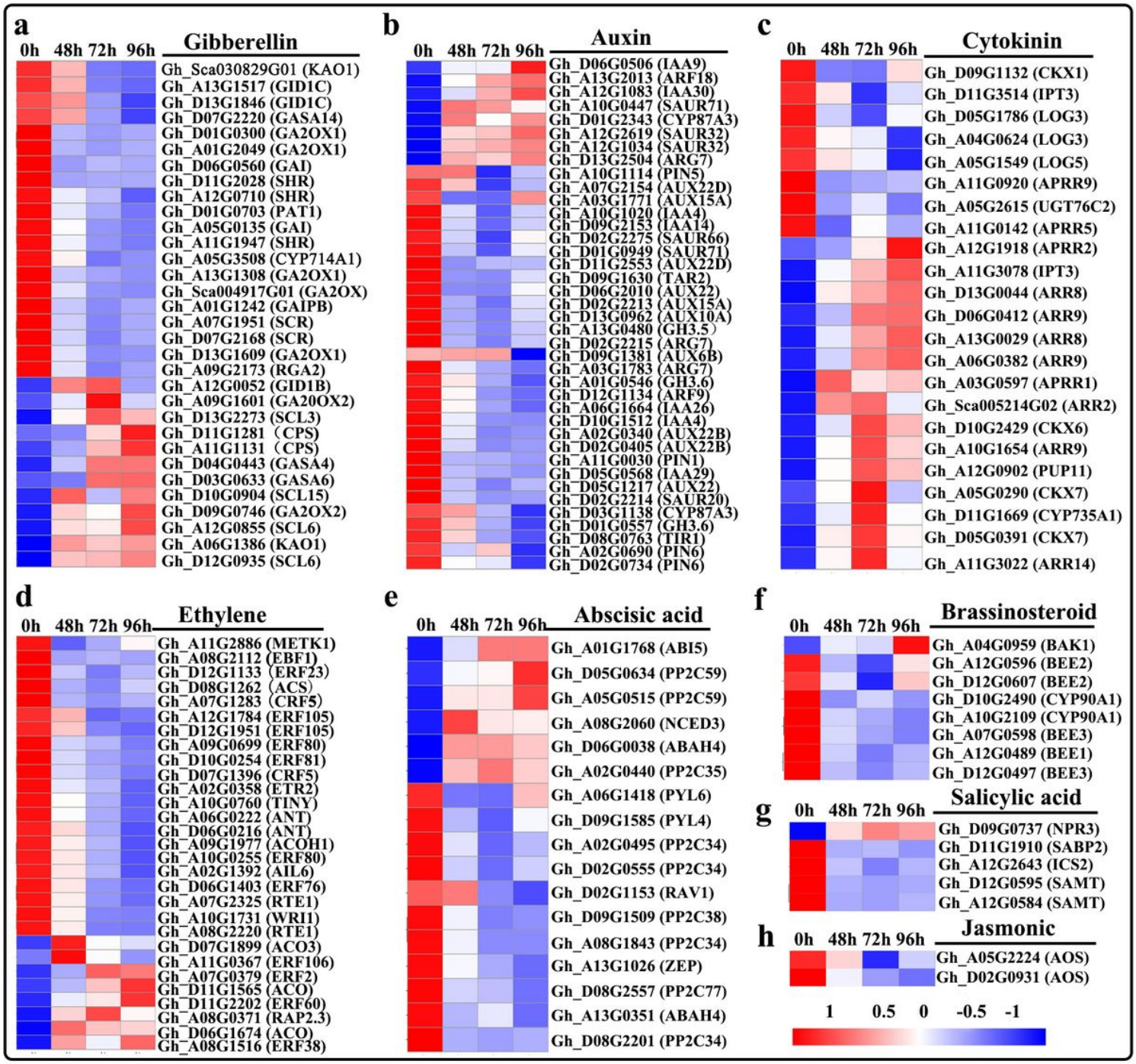

Figure 6

Heatmap of differentially expressed genes related to cell cycles, cell wall biosynthesis and modification, and aquaporins in the second internode between MC treatment and control. Gene expression level (FPKM) was normalized with Z-score. Blue indicates lower expression, and red indicates higher expression. 0 h: Control; 48, 72 and 96: 48 h, 72 h and 96 h after MC-treatment.

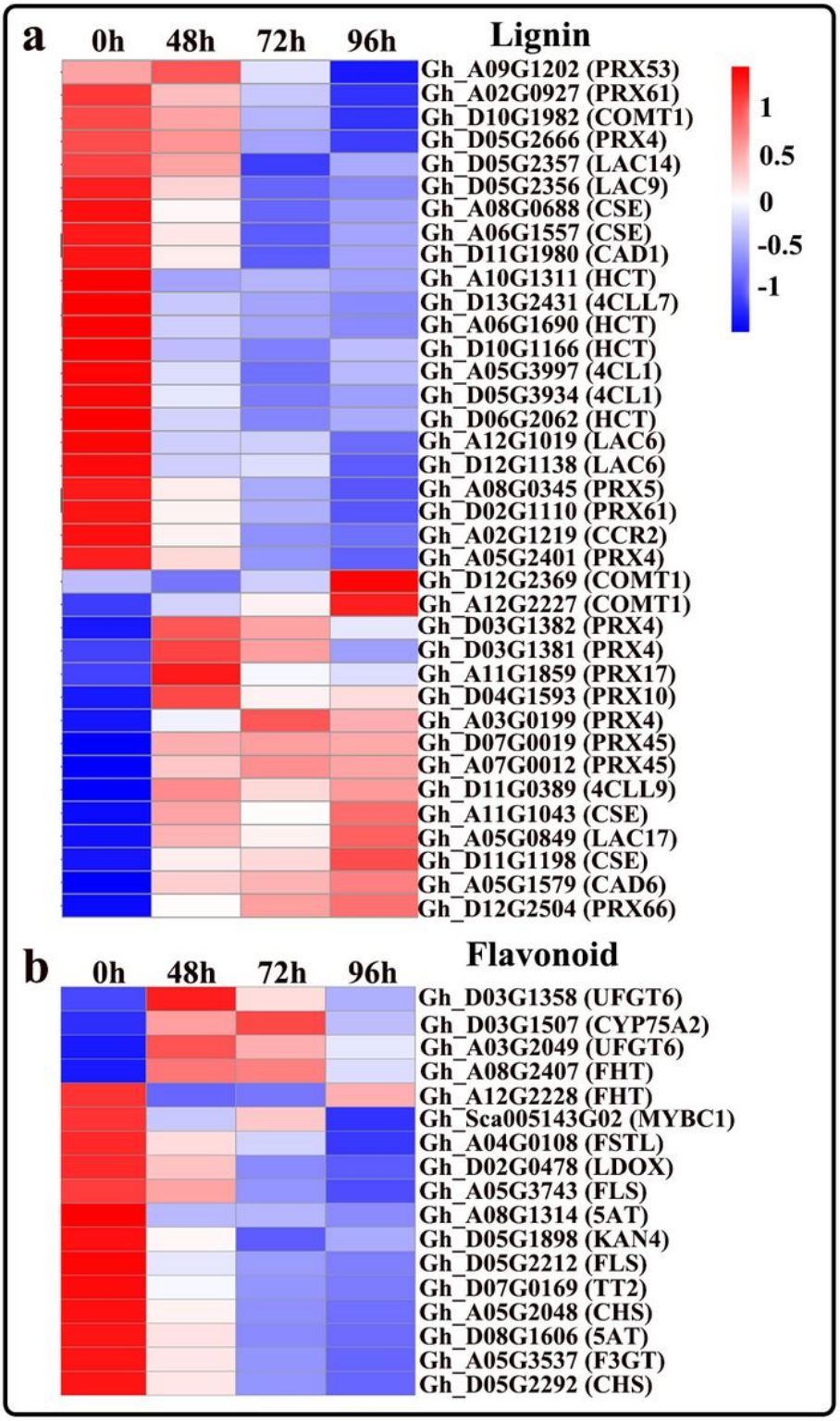

Figure 7

Heatmap of differentially expressed genes involved in lignin and flavonoid metabolism in the second internode between MC treatment and control. Gene expression level (FPKM) was normalized with Z-score. Blue indicates lower expression, and red indicates higher expression. 0 h: Control; 48, 72 and 96: 48 h, 72 h and 96 h after MC-treatment.

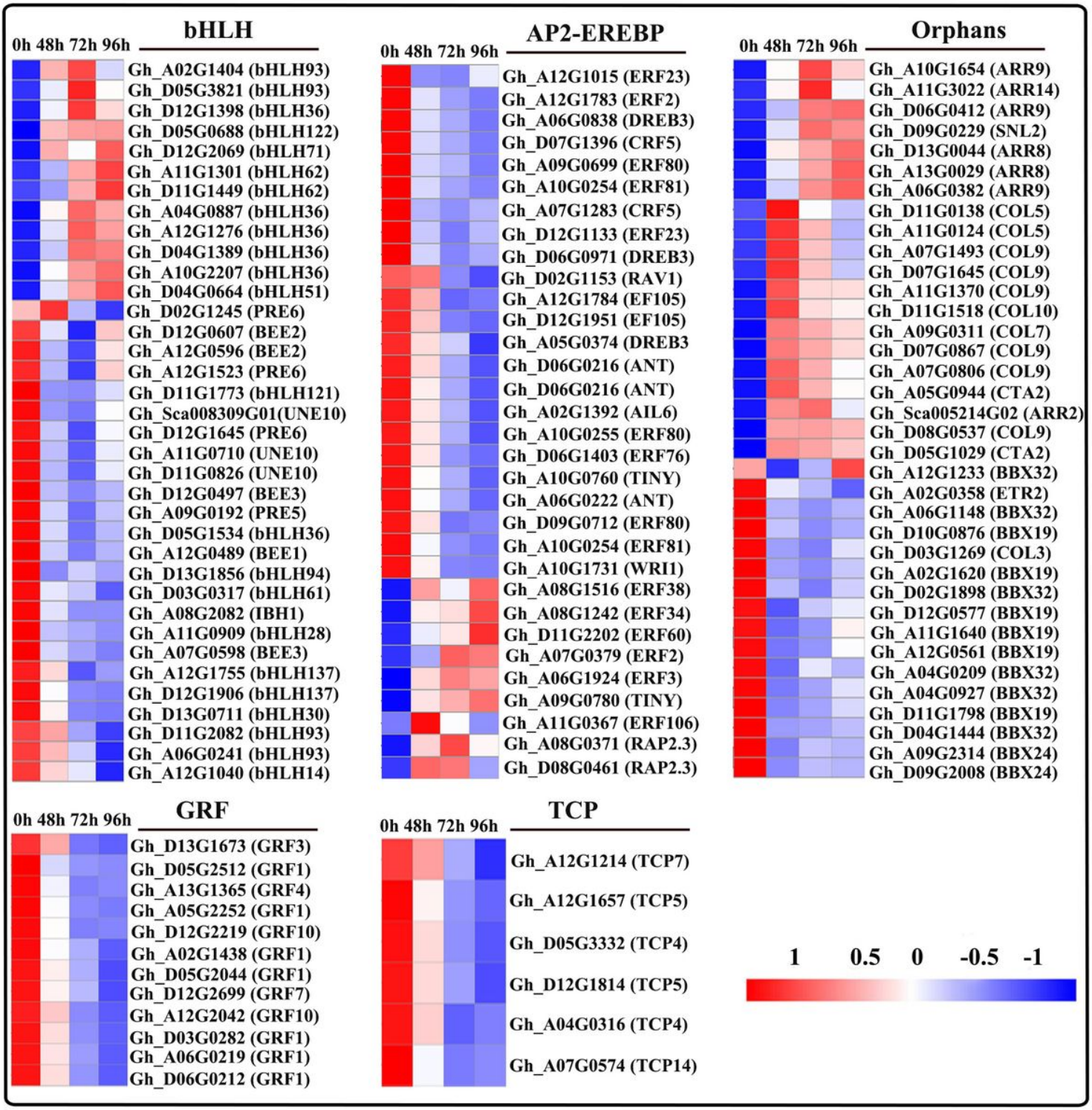

Figure 8

Heatmap of differentially expressed transcription factors in the second internode between MC treatment and control. Gene expression level (FPKM) was normalized with Z-score. Blue indicates lower expression, and red indicates higher expression. 0 h: Control; 48, 72 and 96: 48 h, 72 h and 96 h after MC-treatment.

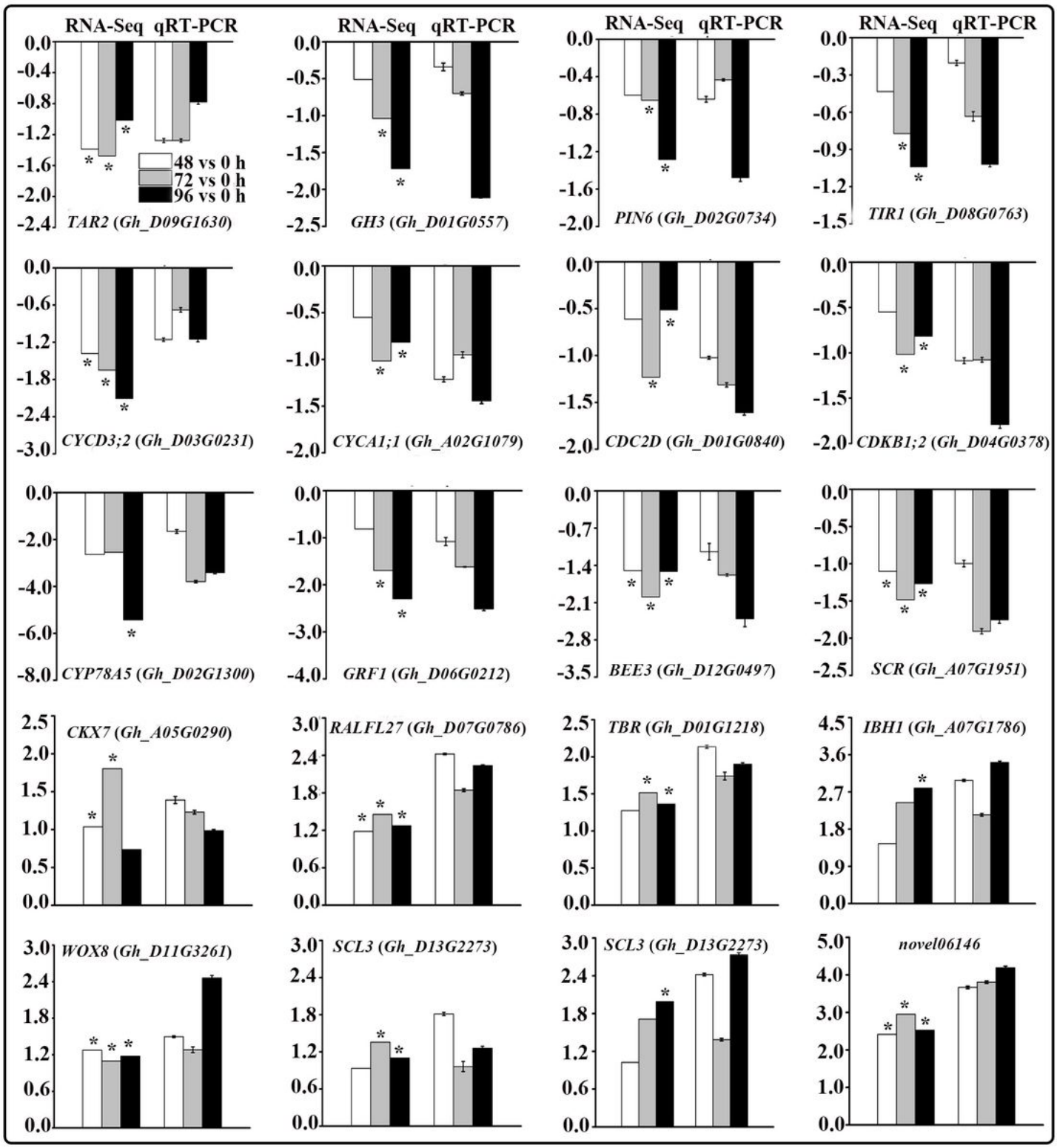

Figure 9

Validation of DEGs from RNA-Seq analysis by quantitative reverse transcription polymerase chain reaction (qRT-PCR). Y-axis represents the log2 fold change values at 48 h, 72 h and 96 h after MC treatment compared to control (RNA-Seq), or -delt delt Ct (qRT-PCR). Each column represents mean ± SD.* indicates significantly regulated by RNA-Seq analysis.

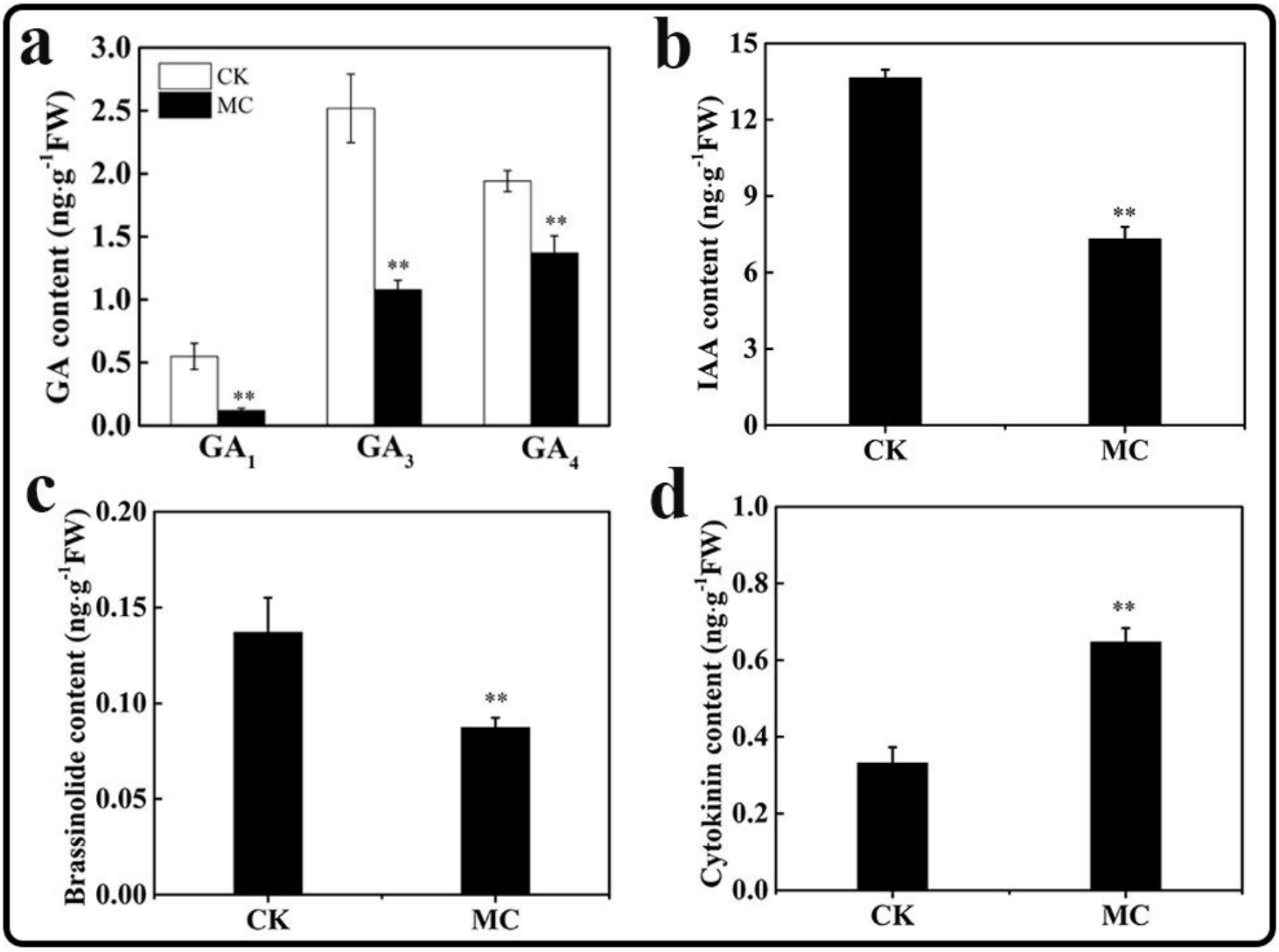

Figure 10

Effects of MC treatment on the contents of endogenous phytohormone in the second internode of cotton seedlings 6 days after treatment. (a) GA1, GA3 and GA4, (b) IAA, (c) brassinolide and (d) cytokinin. **P < 0.01, Student's t-test.

Supplementary Files

This is a list of supplementary files associated with this preprint. Click to download.

- Additionalfile2FigureS2.jpg
- Additionalfile10TableS8.pdf
- Additionalfile1FigureS1.jpg
- Additionalfile3TableS1.xlsx
- Additionalfile4TableS2.xlsx

- Additionalfile6TableS4.xlsx
- Additionalfile5TableS3.xlsx
- Additionalfile8TableS6.xlsx
- Additionalfile7TableS5.xlsx
- Additionalfile9TableS7.xlsx